Analysis of S-N data for new and corroded mooring chains at varying mean load levels using a hierarchical model

Erling N. Lone[a,*], Philippe Mainçon[b], Øystein Gabrielsen[c], Thomas Sauder[b,a], Kjell Larsen[a,c], Bernt J. Leira[a]

[a]*Department of Marine Technology, Norwegian University of Science and Technology, Trondheim N-7491, Norway*
[b]*SINTEF Ocean, P.O. Box 4762 Torgarden, 7465 Trondheim, Norway*
[c]*Equinor ASA, Arkitekt Ebbells veg 10, 7053 Ranheim, Norway*

Abstract

Results from full scale fatigue tests of offshore mooring chains are considered. The data set includes new and used chains, tested at a range of mean load levels. The used chains have been retrieved after operation offshore and include samples with varying surface conditions, ranging from as-new to heavily corroded. Based on a parameterized S-N curve intercept parameter, the effects of mean load and chain condition are estimated empirically by regression analysis. A hierarchical model is used, to properly account for and quantify correlations within subsets of the data. Results show that the mean load and corrosion effects are both significant. Differences in the fatigue performance of new versus used chains are quantified and discussed. The paper also includes an assessment of the impact from correlations between chain links on the fatigue capacity and reliability of a chain segment.

Keywords: Studless chain, S-N analysis, Hierarchical linear model, Mean load, Corrosion, Fatigue reliability

---

1. Introduction

The S-N approach to tension-tension fatigue of mooring chain is considered. Capacity curves for fatigue assessment of mooring chain components are then traditionally given of the form [1]

$$N = A \cdot S^{-m} \tag{1}$$

where N is the number of cycles to failure at stress range S [MPa], A is referred to as the intercept parameter and m is referred to as the slope parameter.[1] In logarithmic space, the curve is given by

$$\log N = \log A - m \cdot \log S \tag{2}$$

where $\log(\cdot)$ usually refers to the common logarithm in relation to S-N data. The parameters A and m are estimated by fitting Equation (2) to the results of constant amplitude tests performed at various stress range levels, typically by use of linear regression analysis [4].

The parameters of current fatigue design curves for mooring chain [1, 3] are based on full scale tests for new chain, performed at a mean load of 20% of the minimum breaking load (MBL) [5]. In fatigue calculations following the procedure outlined by the standards, degradation due to corrosion is accounted for

---

*Corresponding author.
Email address: erling.lone@ntnu.no (Erling N. Lone)

[1]For mooring chain, a stress-based assessment according to Equation (1) is prescribed by DNVGL-OS-E301 [1], whereas "T-N" curves based on tension ranges normalized with respect to the breaking strength of a reference quality chain is required by API-RP-2SK [2]. See also [3, Section 9]. For the present study, focus is on the S-N definition.

in a simplified manner by a reduction of the cross section area of the chains – representing the general material loss caused by corrosion – giving an increase in the effective stress ranges entering the calculations. Actual mean tension loads in the mooring lines are disregarded. However, fatigue tests performed in recent years for used chains retrieved after operation offshore [5–11] have revealed that (i) increased surface roughness and pits caused by corrosion have a detrimental effect on the fatigue capacity, and this effect is larger than that obtained from the simplified correction prescribed by the standards; (ii) the fatigue capacity is strongly dependent on the mean load, so that mooring chains tested at lower mean loads performed better than chains tested at higher mean loads with similar degree of corrosion. The positive effect of a lower mean load has been reported also from full scale tests of new chain [12, 13] and from numerical computations [14, 15].

As it stands, the S-N relation in Equation (1) suggests that for a given set of the parameters (A, m) the fatigue capacity depends solely on the stress range. Properly addressing mean load and corrosion effects then requires the use of an effective stress range that implicitly takes these into account. With regards to corrosion, stress concentration factors could be used to scale the stress ranges to represent corrosion effects more realistically than that obtained by a mere reduction of the cross section. However, quantification of such factors would not be straightforward under the S-N assumption.

Empirical correction models for the mean load effect on fatigue exist in the literature. Examples of such are the Gerber, Goodman, Morrow or Smith-Watson-Topper models, see e.g., [16, 17]. These models may be used to transform the stress range applied at a given, non-zero mean stress level to an equivalent stress range that has the same fatigue effect at zero mean stress. The same correction model could then be used to further transform the equivalent stress range to a reference mean stress for which the relevant S-N curve is given (i.e., typically 20% MBL for mooring chain). However; the validity of these correction models for fatigue of mooring chain is questionable. See Gabrielsen et al. [11] for a discussion on this matter.

To account for the effects of both mean load and corrosion, Lone et al. [18] expressed the intercept parameter as a function of mean load and chain condition:

$$\log A(\sigma_m, c) = B_0 + B_1 \cdot g_1(\sigma_m) + B_2 \cdot g_2(c) \tag{3}$$

where $(B_j)_{j\in\{0,1,2\}}$ are coefficients; σ_m is the nominal mean stress; c is a *corrosion grade* describing the condition of the chain on a custom scale from 1 (as new) to 7 (severe corrosion); and $g_1(.)$ and $g_2(.)$ are monotonically increasing functions of σ_m and c, respectively, which are parameter-free and chosen *a priori* (this is addressed later in Section 3 of the present paper). The coefficients of the model were then estimated empirically from a database consisting of full scale fatigue tests for new and used chains, using least-squares regression. Mendoza et al. [19] used the same corrosion grade scale as a measure for chain condition (c), and quantified its effect by considering a S-N model similar to that described by Equations (1) and (3). They used a hierarchical model for the regression analysis, to account for correlations between samples within subsets of the test database.

The present paper unites the works presented in [18] and [19] by (i) estimating empirically both mean load and corrosion effects, and (ii) using a hierarchical model for the regression analysis. Furthermore, the test database used for the present study has been extended through inclusion of additional fatigue tests performed at a range of mean load levels for both new and used chain.

The paper is organized as follows. In Section 2, we describe the fatigue test database and review the corrosion grade scale. In Section 3, we describe the data analysis method. In Section 4, results are presented and discussed. In Section 5, we present and discuss the impact of the results obtained for the hierarchical model on the fatigue capacity and reliability by comparison to results from previous studies. Conclusions are given in Section 6.

2. Fatigue test data

2.1. Test database

The following attributes are common for all the tests included in the present study:

- All tests are for studless chain.
- All tests were performed in seawater.

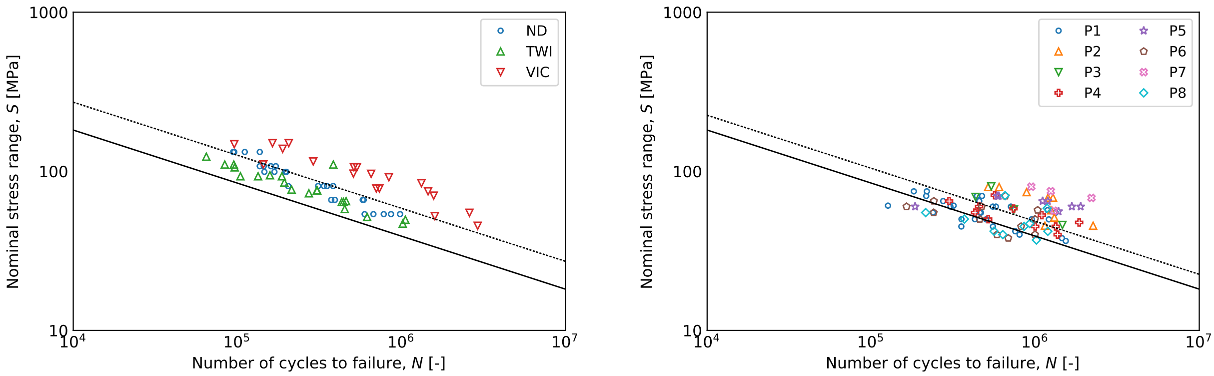

Figure 1: S-N data from fatigue tests for new chain (left) and used chain (right). Mean curve ($m = 3$) for data in each plot (dashed line) and DNVGL-OSE-301 design curve (solid line) are included for reference.

- Only first fractures are included (i.e., continued tests to obtain failure in additional links are not considered).

An overview of the tests is given in Table 1. The new chain tests have been provided from three previous projects: the Noble Denton (ND) joint industry study on 76 mm studless chain of grade R3 and R4 [20]; the TWI joint industry project on fatigue performance of high strength and large diameter studless chain [12]; and a Vicinay (VIC) study on the fatigue performance of R4 and R5 chains for a range of diameters [13, 21].

The used chains have been retrieved by Equinor after service at eight different platforms in the North Sea, and then tested at constant amplitude cyclic loading until failure (corresponding to the notation P1 to P8 in Table 1). Results from several of these tests have previously been published in [5–9, 11]. These samples cover a variety of diameters and chain conditions – see listed references for additional details where available. Note that: (i) The used chain samples have been visually inspected for presence of fatigue cracks prior to testing, and no such cracks have been observed (prior to tests). (ii) A corrosion grade has been assigned to each of the used chain samples, as a quantitative measure of its surface condition. This is elaborated subsequently.

In the table, the tests from each project and platform have been divided into subsets referred to herein as "batch". A general rule used to define these subsets has been to distinguish between different chain sizes (diameter) and material grades (R3/R4/R5). This general rule is inadequate for the data from Vicinay, consisting of samples with a number of unique diameters. Subsets have therefore been defined somewhat inconsistently based on material grade only for this data.

For most of the platforms (P2-P8), the general rule ensures that used chain samples retrieved from different positions along the mooring lines (e.g., top or bottom chain) and after the same service life duration are grouped into different subsets. For one of the platforms (P1), the top and bottom chains are of the same diameter and the samples have been retrieved at various points in time. The subsets defined for this platform have therefore been further refined based on service life and time of retrieval.

A difference across subsets which is not reflected in the table is the number of links included in the test rig for each of the tests. The ND tests were conducted with 7 links; TWI tests were conducted with 7 links for 127 mm chain and 11 links for 76 mm chain; Vicinay's setup ranged from 2 to 9 links; and the used chain tests varied between 3 and 6 links, with 5 links for the majority of the tests.

Figure 1 shows S-N plots of the test data included in the present study. Compared to the new chain data, which vary only in terms of stress range and mean load, the used chain data shows a larger horizontal scatter at each stress range level due to the additional variation of chain condition. For S-N plots distinguishing between mean load and corrosion grade levels for the used chain data, see [18].

Table 1: Overview of full scale fatigue tests included in the data analysis. Total number of tests is 154 (new chain: 67 tests, used chain: 87 tests). Diameter and MBL are nominal values. "Condition" is the corrosion grade assigned.

Project, Platform	Batch[a]	#tests	Material grade	Diameter[b] [mm]	MBL[b] [kN]	Mean load[b] [% MBL]	Condition (1-7)	Service life [years]	Ref.
ND	ND-R3-76	14	R3	76	4884	20.0	1	–	[20]
	ND-R4-76	12	R4	76	6001	20.0	1	–	[20]
TWI	TWI-R4-76	3	R4	76	6001	20.0	1	–	[12]
	TWI-R4-127	3	R4	127	14955	20.0	1	–	[12]
	TWI-R5-76	3	R5	76	7008	20.0	1	–	[12]
	TWI-R5-127	13	R5	127	17465	10.0, 20.0	1	–	[12]
VIC	VIC-R4	7	R4	[102, 171]	[10216, 24292]	[7.9, 14.7]	1	–	[13, 21]
	VIC-R5	12	R5	[70, 165]	[6021, 26833]	[6.7, 14.4]	1	–	[13, 21]
P1	P1-R4-114a	6	R4	114	12420	16.0	2, 5, 6	10	[5–7]
	P1-R4-114b	4	R4	114	12420	[15.7, 16.9]	5	13	–
	P1-R4-114c	5	R4	114	12420	[16.7, 20.0]	5, 6	12	[5, 9]
	P1-R4-114d	4	R4	114	12420	[16.8, 18.0]	4	20	–
	P1-R4-114e	10	R4	114	12420	8.0, 18.0	7	12	[11]
P2	P2-R4-142	9	R4	142	18033	14.0	1	12	[7]
P3	P3-R4-138	4	R4	138	17199	14.0	1	7	–
P4	P4-R4-126	4	R4	126	14775	13.5	2	12	[5, 6]
	P4-R4-136	7	R4	136	16785	11.9	5, 7	19	[5, 8]
P5	P5-R4-130	8	R4	130	15559	6.4, 20.0	5, 6, 7	20	[5, 9]
P6	P6-R3-137	9	R3	137	13829	13.4	4, 7	18	–
	P6-R4-114	3	R4	114	12420	[15.7, 16.8]	4	5	–
P7	P7-R4-145	4	R4	145	18665	9.7	1	15	[5, 7]
P8	P8-R4-130	3	R4	130	15559	17.0	2	16	–
	P8-R4-139	7	R4	139	17407	16.0	5, 7	19	–

[a] Batch identifier, general rule: <project/platform>–<material grade>–<diameter>. See text for additional comments.
[b] Comma-separated values without brackets list all unique entries for the given batch, whereas bracketed values are [min, max].

2.2. Corrosion grade scale

Surface condition for each of the used chain samples has been assessed and graded according to the scale given in Table 2. Examples of graded chain links are shown in Figure 2. A shortcoming of this scale is the inevitable subjectivity involved, making its usage vulnerable to inconsistent categorization. Assessment of the samples used for the present study has therefore been performed by a small group of corrosion experts, to ensure that the corrosion grade scale is applied consistently across samples.

Gabrielsen et al. [11] present preliminary results from ongoing work, aiming to develop computer algorithms that may be used to determine the corrosion grade based on 3-D scans of the chain links. More work is needed for this approach to prove its robustness. However; if successful, future assessment of surface condition may be based on objective algorithms, in lieu of the subjective assessment on which the current study relies.

Table 2: Description of corrosion grades.

Grade	Surface condition
1	New chain, or mild corrosion.
2	Some scattered local corrosion (pitting), less than 1 mm deep.
3	Larger areas effected, local corrosion (pitting) around 1 mm deep.
4	Large areas affected by pitting, 1-3 mm deep, the deeper sharper in nature.
5	Severe and widespread pitting, up to 4 mm deep, but somewhat less than grade 6.
6	Severe and widespread pitting, 3-6 mm.
7	Severe and widespread pitting, 3-6 mm and deeper. Sharp and deep pitting.

2.3. Joint occurrences of mean load and corrosion grade

Since the fatigue test results will be used to estimate empirically the mean load and corrosion grade effects, it is of interest to examine the joint occurrences of these attributes within the test database. This is

(a) Grade 1. (b) Grade 2. (c) Grade 4. (d) Grade 7.

Figure 2: Examples of corrosion grades [18].

presented in Figure 3. The combination of corrosion grade 1 and mean load 20% MBL is the most common (47 tests), since all ND tests and all but one test from TWI were performed at this mean load level. For used chain, a fairly large share of the tests are for corrosion grade 1–2 with a mean load of around 14% MBL (17 tests), and for corrosion grade 4–6 with a mean load around 16–18% MBL (23 tests). It should further be noted that there are no tests with corrosion grade 2–4 combined with a mean load below 14% MBL, only two tests with a corrosion grade above 1 combined with a mean load of 20% MBL, and no tests with mean load above 20% MBL.

Compared to the data used for the study presented in [18], the database has been enriched with more tests at mean loads below 20% MBL. The Vicinay data [13, 21] adds 19 tests for new chain (corrosion grade 1) with mean load in the range from 6.7% to 14.7% MBL, and the subset P1–R4–114e [11] adds 10 tests with corrosion grade 7 at mean loads 8% and 18% MBL (5 tests at each level).

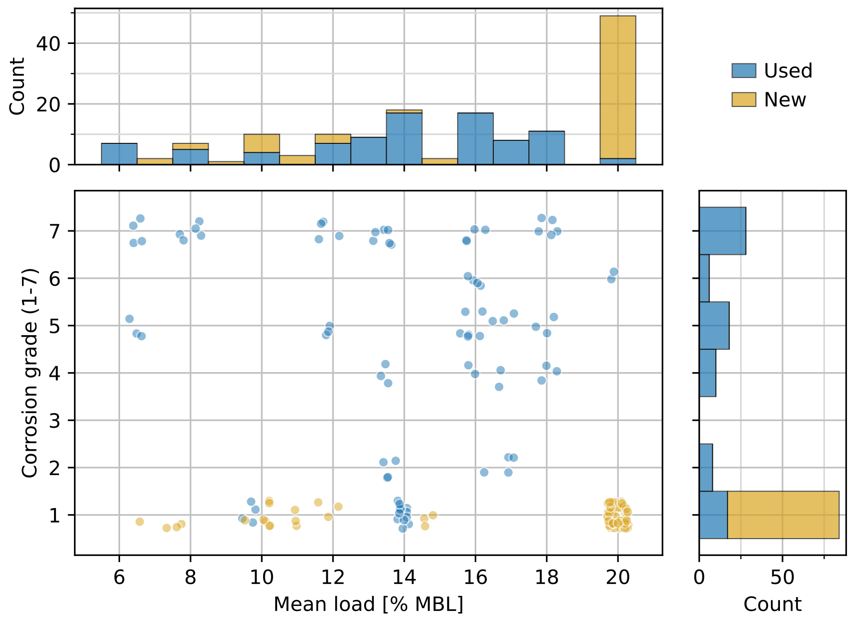

Figure 3: Combinations of mean load and corrosion grade in database, and marginal histograms. Scatter plot data has been jittered (up to ±0.3 in both directions).

3. Data analysis

The data analysis method is now described, including assumptions and limitations to the present study and choice of grouping criterion for the hierarchical model. We will largely follow the notation used by Gelman and Hill [22], which is the main reference for the parts concerned with hierarchical models.

3.1. Assumptions and limitations

The following assumptions and limitations apply to the present study:

1) The study is limited to considering stress range effect fixed at $m = 3$.
2) Prior fatigue loads and damage accumulated during service life are disregarded.
3) Differences in number of links in the test rigs are neglected. All test results are assumed to represent failure of a single link.
4) Nominal stress ranges are considered. An implicit assumption is thus that the loss of cross section area due to corrosion is negligible, and that the effect of corrosion pits and increased surface roughness is fully represented by the corrosion grade.

The consequences of these assumptions are discussed in Section 4.

3.2. Motivation for using a hierarchical model

Classical regression under the assumption of normal distributed errors may be expressed as

$$\begin{aligned} y_i &= \beta_0 + \boldsymbol{x}_i\boldsymbol{\beta} + \epsilon_i, \qquad \text{for } i = 1, \dots, n \\ \epsilon_i &\sim N(0, \sigma_\epsilon^2) \end{aligned} \tag{4}$$

where y_i is the number of cycles to failure in the test of the i^{th} sample, β_0 is the intercept, $\boldsymbol{\beta} = (\beta_1, \dots, \beta_p)$ is a column vector with slope coefficients, $\boldsymbol{x}_i = (x_{i1}, \dots, x_{ip})$ is a row vector containing predictors, and ϵ_i is the model error. The model in (4) implies that the errors are assumed to follow *independent* normal distributions, $\epsilon \sim N(\mathbf{0}, \sigma_\epsilon^2\boldsymbol{I})$, where σ_ϵ is referred to as the standard error of the model and $\boldsymbol{I}$ is the $n \times n$ identity matrix. However; if it is natural to sort the samples into groups (e.g., based on different size, material grade or other attributes that vary across subsets), the data may be clustered, with correlated errors. This is referred to as a hierarchical data structure, and it may then be incorrect to assume that the data points (and thus, the errors) are independent. When faced with hierarchical data, two extreme alternatives for the regression analysis are:

- *Complete pooling:* fit a single model according to (4), ignoring the hierarchical structure of the data. This may lead to underfitting, with biased estimates for the model coefficients and possibly poor predictive performance for new (unseen) observations.
- *No pooling:* fit separate models, applying the regression model in (4) to each group of data separately. This may lead to overfitting and high variance estimates for the coefficients, unless each group contains a sufficient amount of data (which is not the case in many practical problems). Furthermore, this approach (i) does not allow to enforce that groups may be sharing some of the parameters of the model (e.g., one or more of the slope coefficients), and (ii) is inadequate for predicting new observations in new (unseen) groups.

A less extreme version of the no-pooling approach is obtained by adding categorical predictors for each group to the complete-pooling modeling. In this case, the single regression model defined in (4) is adjusted as follows: the common intercept (β_0) is omitted, and one predictor is added per group with an indicator value that is either 1 (if the sample is a member of the corresponding group) or 0 (otherwise). This allows enforcing shared slope coefficients across groups while estimating separate intercept parameters, but will still yield high-variance estimates and be inadequate for prediction of observations from new groups.

Regression analysis by use of a hierarchical model is referred to as *partial pooling*, and is a compromise between these extreme approaches. It combines the data from all groups, thereby maximizing the information extracted from the data, while avoiding the issues of over- or underfitting the model. Also, the resulting model may be used for predictions of new observation in both existing and new groups.

3.3. Regression analysis with hierarchical model

The focus for the present study is on the model

$$\begin{aligned} y_i &= \alpha_{j[i]} + \boldsymbol{x}_i \boldsymbol{\beta} + \epsilon_i \\ \epsilon_i &\sim N(0, \sigma_\epsilon^2) \\ \alpha_j &\sim N(\mu_\alpha, \sigma_\alpha^2) \end{aligned} \tag{5}$$

where $j \in (1, \ldots, J)$ is a group index, $j[i]$ denotes group membership for the i^{th} sample, and α_j is the group intercept. This type of model is called a varying-intercept model, and the model parameters are $(\alpha_1, \ldots, \alpha_J, \beta_1, \ldots, \beta_p, \sigma_\epsilon, \mu_\alpha, \sigma_\alpha)$, but not ϵ_i. A particularity of this model is that both the group intercepts, α_j (data-level parameters), and the parameters μ_α and σ_α of the distribution of these intercepts (higher-level parameters), are parameters of the model: they are all estimated in a maximum likelihood procedure, or have their distributions updated in Bayesian inference.

An equivalent way of writing the model is

$$\begin{aligned} y_i &= \mu_\alpha + \eta_{j[i]} + \boldsymbol{x}_i \boldsymbol{\beta} + \epsilon_i \\ \epsilon_i &\sim N(0, \sigma_\epsilon^2) \\ \eta_j &\sim N(0, \sigma_\alpha^2) \end{aligned} \tag{6}$$

where η_j is the group-level error. In other words; compared to the classical regression model, the hierarchical model splits the model error into two terms such that σ_ϵ describes the standard deviation of data-level errors (i.e., within-group variations) and σ_α is the group-level standard error (i.e., between-group variations).[2] This implicitly allows for modeling of correlations within groups, and will be utilized later (Section 5) to assess the effect of within-group correlations on the fatigue capacity of a chain segment.

Return now to the model in (5). Let $\theta = (\alpha_1, \ldots, \alpha_J, \beta_1, \ldots, \beta_p, \sigma_\epsilon)$ denote the data-level parameters, and let $\omega = (\mu_\alpha, \sigma_\alpha)$ denote the higher-level parameters. Using Bayes' rule, the joint posterior distribution of θ and ω may be expressed as [24]:

$$\begin{aligned} p(\theta, \omega | y) &\propto p(y | \theta, \omega) \cdot p(\theta, \omega) \\ &= p(y | \theta, \omega) \cdot p(\theta | \omega) \cdot p(\omega) \end{aligned} \tag{7}$$

where $p(\cdot\,|\,\cdot)$ denotes a conditional probability density, $p(\cdot\,,\cdot)$ denotes a joint density and $p(\cdot)$ denotes a marginal density. For notational convenience we have here omitted the dependence on the predictors, $\boldsymbol{x}$. From (5) we see that for a given value of θ, the data distribution does not depend on ω, meaning that $p(y|\theta, \omega) = p(y|\theta)$. Equation (7) may then be written as:

$$p(\theta, \omega | y) \propto p(y | \theta) \cdot p(\theta | \omega) \cdot p(\omega) \tag{8}$$

where $p(y\,|\,\theta)$ is the likelihood of the data given the data-level parameters; $p(\theta\,|\,\omega)$ is referred to as the *population distribution*; $p(\omega)$ is the *hyperprior distribution*; and $p(\theta, \omega) = p(\theta|\omega) \cdot p(\omega)$ is referred to as the *joint prior distribution* [24, Chapter 5]. The likelihood function is

$$p(y|\theta) = \prod_{i=1}^{n} N(y_i\,|\,\alpha_{j[i]} + \boldsymbol{x}_i \boldsymbol{\beta},\, \sigma_\epsilon^2) \tag{9}$$

where $N(y_i\,|\,\mu, \sigma^2)$ denotes a normal probability density function with mean μ and variance σ^2, evaluated for y_i. Assuming *a priori* independence between $(\boldsymbol{\beta}, \sigma_\epsilon)$ and the remaining parameters, the population distribution is:

$$p(\theta|\omega) = p(\boldsymbol{\beta}, \sigma_\epsilon) \cdot \prod_{j=1}^{J} N(\alpha_j\,|\,\mu_\alpha, \sigma_\alpha^2) \tag{10}$$

[2]The model in (5) or (6) is sometimes called a *linear mixed-effects model*, with α_j (or η_j) referred to as *random* effects and $\boldsymbol{\beta}$ referred to as *fixed* effects. See e.g., [23].

which shows that under the model in (5), we regard each group intercept α_j as a realization from a *common* distribution, $N(\mu_\alpha, \sigma_\alpha^2)$. This has the effect of constraining them, so that they are pulled towards a common mean value (μ_α) compared to if they were estimated solely from the data within each group. Furthermore, it implies that the group-specific intercepts are informed by data across all groups, since all data points inform the posterior distribution of the higher-level parameters. For further details, see [22, Chapter 18], [24, Chapters 5 and 15] or [25, Chapter 9].

In the following paragraphs we briefly describe the implementation for the present study, as well as aspects of the hierarchical model that are of relevance for the work presented herein.

Estimation of model parameters. For the present work, the model parameters are estimated by using the Python module `statsmodels` [26] and its `MixedLM()` class, which is an implementation of the restricted maximum likelihood procedure described in [23]. The point estimates obtained correspond to the Bayesian posterior modes of the parameters based on (8) with flat priors for $\boldsymbol{\beta}$, σ_ϵ, μ_α and σ_α.

Amount of pooling and standard error of $\hat{\alpha}_j$. Given the data and the remaining model parameters, the inferences for the group intercepts follow independent normal distributions [22, p. 394]:

$$\hat{\alpha}_j | y, \boldsymbol{\beta}, \sigma_\epsilon, \mu_\alpha, \sigma_\alpha \sim N(\hat{\alpha}_j, V_j) \tag{11}$$

where $\hat{\alpha}_j$ is the posterior mean of α_j and V_j is the estimation variance, given by

$$\hat{\alpha}_j = V_j \left(\frac{n_j}{\sigma_\epsilon^2} (\bar{y}_j - \bar{\boldsymbol{x}}_j \boldsymbol{\beta}) + \frac{1}{\sigma_\alpha^2} \mu_\alpha \right), \quad V_j = \left(\frac{n_j}{\sigma_\epsilon^2} + \frac{1}{\sigma_\alpha^2} \right)^{-1} \tag{12}$$

where n_j is the number of samples in group j, $\bar{y}_j$ is the mean of the outcomes for group j, $\bar{\boldsymbol{x}}_j$ is a vector containing the means of the predictors for this group. This shows that (i) for groups with sample size $n_j < \sigma_\epsilon^2/\sigma_\alpha^2$, the estimated intercept is closer to μ_α than to the unpooled estimate that would be obtained from group-specific information only (i.e., $\bar{y}_j - \bar{\boldsymbol{x}}_j \boldsymbol{\beta}$); (ii) for groups with $n_j > \sigma_\epsilon^2/\sigma_\alpha^2$, the group-specific information is more important than μ_α; and (iii) the uncertainty in $\hat{\alpha}_j$ decreases with increasing group sample size, n_j.

Relation to complete-pooling and no-pooling models. As described in relation to (10), the common population distribution constrains the inferences of the group intercepts. Equation (12) shows that this effect may be viewed as a soft constraint, where the amount of pooling depends on the model errors and the number of data points in each group. Let us now consider a hypothetical case, in which we change the model as follows: instead of estimating the value of σ_α from the data (by applying a flat prior for it, as we do in the present study), we *choose* a fixed value for σ_α that we plug into the population distribution in (10). Two special cases are then the following. (i) In the limit that $\sigma_\alpha \to 0$, all group intercepts are forced to the same common value and we have a complete-pooling model. (ii) For $\sigma_\alpha \to \infty$, no constraints apply to α_j and we have a version of a no-pooling model, with unpooled estimates for the group intercepts (but still, pooled estimates for the slope coefficients, $\boldsymbol{\beta}$).

Within-group correlation. The models in (5) or (6) imply that the outcomes (here: fatigue performance) for samples within the same group are correlated with correlation coefficient

$$\rho = \frac{\sigma_\alpha^2}{\sigma_\alpha^2 + \sigma_\epsilon^2} \tag{13}$$

This quantity is also known as the *intraclass correlation* (ICC).

Prediction of new observations. Two scenarios are of relevance for predicting the outcome for a new sample. (i) For a new sample, $\tilde{y}$, from an existing group j, the outcome may be predicted from

$$\tilde{y} \sim N(\alpha_j + \tilde{\boldsymbol{x}}\boldsymbol{\beta}, \sigma_\epsilon^2) \tag{14}$$

where $\tilde{\boldsymbol{x}}$ are the predictor values for the new sample.[3] (ii) For a new sample from a new group (i.e., a group that was not included in the data analysis), the intercept is unknown and must be predicted from $\tilde{\alpha} \sim N(\mu_\alpha, \sigma_\alpha^2)$. This may be expressed as

$$\begin{aligned} \tilde{y} &\sim N(\mu_\alpha + \eta + \tilde{\boldsymbol{x}}\boldsymbol{\beta}, \sigma_\epsilon^2) \\ \eta &\sim N(0, \sigma_\alpha^2) \end{aligned} \tag{15}$$

or, equivalently, as

$$\tilde{y} \sim N(\mu_\alpha + \tilde{\boldsymbol{x}}\boldsymbol{\beta}, \sigma^2) \tag{16}$$

where

$$\sigma = \sqrt{\sigma_\alpha^2 + \sigma_\epsilon^2} \tag{17}$$

is the total standard deviation of the outcome for a new sample from a new group.

3.4. Outcome and predictor variables

The objective of the study is to establish a fatigue capacity curve with dependence to mean load and chain condition. A predictor is therefore included for each of these effects. The stress range would generally also be included as a predictor. However, since we have assumed that the stress range effect is fixed at $m = 3$, it is technically included in the outcome variable instead. The outcome and predictor variables are:

$$\begin{aligned} y_i &= \log N_i + m \cdot \log S_i \\ x_{i1} &= g_1(\sigma_{m,i}) \\ x_{i2} &= g_2(c_i) \end{aligned} \tag{18}$$

where the stress range S has unit MPa, and $g_1(\sigma_m)$ and $g_2(c)$ are functions of the mean stress (σ_m) and corrosion grade (c), respectively. The choice of these functions will be based on findings from the previous study presented in [18], and is described in detail subsequently.

3.5. Grouping criterion

An essential step in setting up the hierarchical model is the choice of a grouping criterion. That is, the attribute or property, or set of such, by which we divide the data into groups $j \in (1, \ldots, J)$. In the following, we will use the terms *controlled*, *non-controlled* and *hidden* variable to describe attributes or properties as follows. (i) A *controlled* variable may be assigned a value of choice in connection with the experimental design of the tests, to make it independent of other variables affecting the outcome (e.g., the stress range of a fatigue test). (ii) A *non-controlled* variable may be measured, but not controlled (e.g., the condition of a sample). (iii) A *hidden* variable is any attribute or property that affects the outcome of the test, directly or indirectly, but is not explicitly included in the regression model (e.g., the material grade or the prior fatigue loads of a sample).

Firstly; hidden variables that influence simultaneously both non-controlled predictors and the test outcome may cause correlations within subsets of the data, resulting in biased estimates for the effects of these predictors. Secondly; in practice, the values of the controlled variables are not necessarily as independent of the hidden variables as one would like them to be, in particular for experimental data as costly as full scale fatigue tests. Hence, ideally, we want any hidden variable to have the same value within each group.

[3] As written here, the predictive distribution for a new sample in an existing group ignores inferential uncertainty and assumes that the coefficients $(\alpha_j, \boldsymbol{\beta}, \sigma_\epsilon)$ are known. In practice, estimated values $(\hat{\alpha}_j, \hat{\boldsymbol{\beta}}, \hat{\sigma}_\epsilon)$ must be used and the inferential uncertainty may be of importance as well.

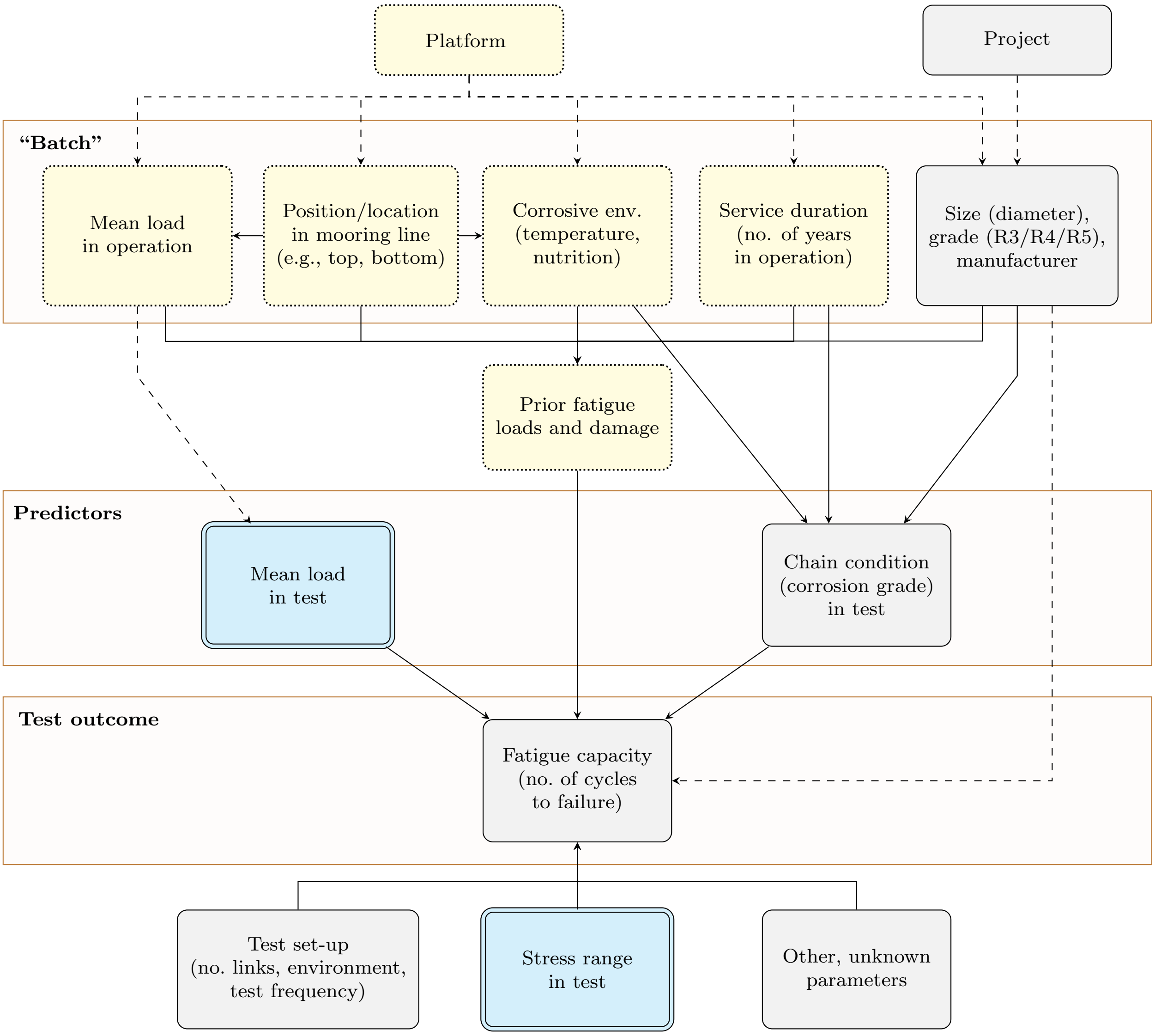

Figure 4: Structure of data and regression model. Grey box: relevance for all tests. Yellow box (dashed border): relevance for used chains only. Blue box (double border): controlled variable in test. Dashed arrow: indirect and/or presumably weak relationship.

A dilemma is, however, that a too strict grouping criterion may result in many groups with few data points each, causing high-variance estimates for the model parameters. Nevertheless, a fairly large number of groups containing few observations is fully acceptable for the hierarchical model [22, p. 276]. In general, increasing the number of samples per group should therefore not be a goal in itself, at the cost of defining a less suitable grouping criterion. This choice should therefore be based on a careful evaluation of available data and the process behind them.

The hierarchical structure of the data used for the present study is illustrated in Figure 4. In this diagram, boxes represent attributes and properties of the sample or the test, whereas arrows indicate direct or indirect relationships. As indicated in the figure, stress range applied in the test is a controlled variable. In principle, so is the mean load applied in the tests. This is largely the case for the new chain tests, and for the latest tests for platform P1 (batch P1-R4-114e, see Table 1). However; for several of the used chain tests, in particular those performed in the early years of the test campaigns, the applied mean load was selected partly based on mean load experienced during operation. It is therefore influenced by hidden variables to some degree for these samples.

Corrosion grade is inevitably a non-controlled variable. It cannot be assigned a value of choice to obtain an optimum experimental design, and is largely influenced by hidden variables such a service duration, position in mooring line (which affects the corrosive environment) and possibly also the material grade and the base material chemistry used by the manufacturer of that particular sample [27]. Moreover; (i) all the hidden variables shown in the second level of Figure 4 influence the fatigue loads and damage accumulated during operation; and (ii) although previous studies for new chain have concluded that there is no significant effect of size and material grade [12, 13, 20], we cannot presume *a priori* that this is the case also for corroded chain.

On this basis, the "batch" criterion defined in relation to Table 1 appears as a reasonable grouping criterion for used chain. This is not to suggest that the prior fatigue loads and damage are the same for used chain within each batch. Rather, division by batch ensures that relevant hidden variables have roughly the same value within each group. Note also that grouping purely by platform may be a poor choice: although the hidden variables for each sample are certainly influenced by the platform at which they were operated, their values may vary largely for samples originating from the same platform. As an example, two chain samples retrieved from the same platform may be from different manufacturers or of different material grades, and may have been exposed to very different mean loads levels or service durations depending on the chain diameters and positions within the mooring line.

Batch is applied as the grouping criterion also for new chain, enabling investigation of group effects related to size and material grade for these samples as well – particularly in relation to different mean load predictors. Note that in doing so, we retain the slightly inconsistent batch definition for the Vicinay data (i.e., based on grade only, ignoring size differences). This is believed to be an acceptable simplification, as new chain samples are presumably less affected by hidden variables compared to used chain.

3.6. S-N intercept

Based on the S-N relation in (2), the predictive distribution in (16) and the predictor variables in (18), the S-N intercept for a sample from a new group has mean value

$$\log A(\sigma_m, c) = \mu_\alpha + \beta_1 \cdot g_1(\sigma_m) + \beta_2 \cdot g_2(c) \tag{19}$$

and standard deviation σ as given in (17). This formulation is consistent with that used in [18], as defined in Equation (3).

According to DNVGL-OS-E301 [1], the *design curve* intercept should be associated with 97.72% probability of exceedance. Under the assumption of normal distributed model errors, this is obtained by subtracting two standard deviations if the model coefficients and σ are known. When these are instead estimated from data, the inferential uncertainty of the estimated coefficients requires a larger offset. This may be expressed as

$$\log A_D(\sigma_m, c) = \hat{\mu}_\alpha + \hat{\beta}_1 \cdot g_1(\sigma_m) + \hat{\beta}_2 \cdot g_2(c) - k_n \cdot \hat{\sigma}, \qquad k_n \geq 2 \tag{20}$$

where subscript $\cdot_D$ denotes design curve value, and superscript $\hat{\cdot}$ implies that an estimate of the parameter is used. The offset k_n depends on the fatigue test sample size (n), and in principle it may also depend on the mean load and corrosion grade level for which the intercept is calculated. The latter dependency is here neglected for simplicity,and the design curve offset is calculated from the empirical function given in [1, Ch. 2, Sec. 2, clause 6.5.4].

A convenient representation of the design curve intercept is obtained by defining a *design* value for μ_α:

$$\hat{\mu}_{\alpha,D} = \hat{\mu}_\alpha - k_n \cdot \hat{\sigma} \tag{21}$$

The design curve intercept is then obtained by substituting $(\hat{\mu}_{\alpha,D}, \hat{\beta}_1, \hat{\beta}_2)$ into (19).

3.7. Description of cases

A summary of the base case considered for the data analysis is presented in Table 3, along with model variations that are applied one at a time. The basis for addressing these particular variations is briefly described here.

Table 3: Overview of base case and model variations.

Model and data	Base case	Variations
Pooling:	Partial pooling	Complete-pooling, no-pooling[a]
Predictors:	$g_1(\sigma_m) = \lambda_m$ [% MBL]	$g_1(\sigma_m) = \sigma_m$ [MPa]
	$g_2(c) = c$	$g_2(c) = \log c$
Data set:	All data	New chain, used chain
Grouping criterion:	Batch	–

[a] Unpooled estimates for group intercepts (α_j), and completely pooled estimates for slope coefficients ($\boldsymbol{\beta}$).

A partial pooling model is the base case. Using batch as the grouping criterion gives $J = 23$ groups with group sizes ranging from 3 to 14 samples per group at an average of $154/23 = 6.7$. For data as scattered as fatigue tests, in particular when exposed to varying mean loads and chain conditions, this amount of data per group may intuitively appear insufficient and associated with a risk of overfitting. To get a sense of how the model performs in this regard besides the measures described previously, and how partial pooling affects the estimated slope coefficients, we will compare to results from complete-pooling and no-pooling models. The complete-pooling estimates are obtained from classical least-squares regression with all data in a single group. The no-pooling estimates are computed by adding categorical variables for groups to the complete-pooling model. This no-pooling implementation is a less extreme version than the no-pooling approach describe in Section 3.2. It does not result in 23 separate models, but a single model with unpooled estimates for group intercepts and completely pooled estimates for the slope coefficients – consistent with the varying-intercept model applied for partial pooling.

Base case predictors are defined based on findings from the previous study presented in [18]. Variation of predictors is here limited to consideration of one alternative function for mean load and corrosion grade effects, respectively. In [18], these alternative predictors did not perform as well as those defined for the base case, however; it is of interest to reassess them in light of the hierarchical model and the extended data set. For an assessment of additional predictor candidates, based on a complete-pooling model, see [18].

The varying-intercept model in (5) assumes that the slope coefficients are the same across groups. That is, that the effects of mean load and chain condition are the same for all groups of data. As a first, small step towards assessing the validity of this assumption for the mean load effect, we apply the partial pooling model separately on new and used chain samples. These results will also serve to quantify possible differences in average intercept and between-group variability for new versus used chain samples.

4. Results and discussion

The results of the data analysis are now presented and discussed. First, regression results for all cases are presented. Selected aspects of the base case and the model variations are thereafter presented and discussed more in detail. The section concludes with a summary of the findings and a discussion on the underlying assumptions.

4.1. Results

Results for all model variations considered are listed in Table 4. From Equation (19) it is seen that the estimated mean intercept, $\hat{\mu}_\alpha$, corresponds to the S-N intercept, $\log A(.)$, for the combination of $g_1(\sigma_m) = 0$ and $g_2(c) = 0$. With the base case predictors this occurs for zero mean load, $\lambda_m = 0$, which is not particularly realistic for operation of mooring chain, and the fictitious corrosion grade $c = 0$. Direct comparison of $\hat{\mu}_\alpha$ across models is thus of limited value, even when identical predictors are used. A more convenient reference

Table 4: Results.

Variation:	Pooling			Predictors		New vs. used chain	
Description:	Partial[a]	Complete	None[b]	Mean load	Corrosion	New	Used
Model no.:	1	2	3	4	5	6	7
Model parameters							
n	154	154	154	154	154	67	87
J	23	1	23	23	23	8	15
$g_1(\sigma_m)$	λ_m	λ_m	λ_m	σ_m	λ_m	λ_m	λ_m
$g_2(c)$	c	c	c	c	$\log c$	–	c
Coefficient estimates and standard errors[e]							
$\hat{\mu}_\alpha$	12.236	12.270	12.177[c]	12.129[d]	12.154[d]	12.150	12.231
$\hat{\beta}_1$	−0.0514	−0.0518	−0.0510	−0.0072[d]	−0.0508	−0.0503	−0.0547
$\hat{\beta}_2$	−0.0977	−0.1052	−0.0783	−0.1003	−0.6616[d]	–	−0.0893
$\mathrm{se}(\hat{\mu}_\alpha)$	0.0811	0.0601	–	0.0851	0.0815	0.1245	0.1034
$\mathrm{se}(\hat{\beta}_1)$	0.0044	0.0033	0.0059	0.0007[d]	0.0046	0.0068	0.0060
$\mathrm{se}(\hat{\beta}_2)$	0.0093	0.0058	0.0200	0.0111	0.0686	–	0.0119
Model errors and ICC							
$\hat{\sigma}_\epsilon$	0.144	0.168	0.144	0.145	0.145	0.142	0.146
$\hat{\sigma}_\alpha$	0.092	–	0.116	0.123	0.104	0.079	0.099
$\hat{\sigma}$	0.171	0.168	0.185	0.190	0.178	0.162	0.176
$\hat{\rho}$	0.29	–	–	0.42	0.34	0.24	0.32
S-N intercept and fatigue life ratio at reference level ($\lambda_m = 20$, $c = 1$)							
$\log A_{\mathrm{ref}}$	11.111	11.129	11.079	–	11.138	11.144	11.048
N_{ratio}	1.00	1.04	0.93	–	1.06	1.08	0.87
Design curve values							
k_n	2.02	2.02	2.02	2.02	2.02	2.05	2.04
$\hat{\mu}_{\alpha,D}$	11.891	11.931	–	11.744	11.794	11.817	11.872
$\log A_{D,\mathrm{ref}}$	10.766	10.790	–	–	10.778	10.811	10.689
$N_{D,\mathrm{ratio}}$	1.00	1.06	–	–	1.03	1.11	0.84

[a] Base case.
[b] No-pooling model with unpooled estimates for group intercepts and pooled estimates for slope coefficients.
[c] For no-pooling model, μ_α is here calculated as weighted mean of group intercepts (weighted by no. of samples per group).
[d] Not directly comparable to base case estimate due to differing predictor unit(s).
[e] Standard errors for coefficients are denoted by se(.).

level is the combination of $\lambda_m = 20$ and $c = 1$. That is, new (or as new) chain operated at a mean load of 20% MBL, which is consistent with the current design curves given in standards. The S-N intercept for this reference level is denoted A_{ref} in Table 4.

Another useful measure for comparison across models is the fatigue life ratio, defined as:

$$N_{\mathrm{ratio}} = \frac{A_{\mathrm{ref}}}{A_{\mathrm{ref}}^{(\mathrm{basecase})}} = 10^{\log A_{\mathrm{ref}} - \log A_{\mathrm{ref}}^{(\mathrm{basecase})}} \tag{22}$$

where $A_{\mathrm{ref}}^{(\mathrm{basecase})}$ is the reference value calculated from the base case model (partial pooling with base case predictors). Hence, N_{ratio} expresses the estimated fatigue capacity for a given model, at the reference level, relative to the base case model.

Finally, design curve values are also given in the table. These serve two main purposes: (i) they enable comparison across models accounting for differences in model errors, and (ii) the design curve intercept for the reference level, $\log A_{D,\mathrm{ref}}$, is directly comparable to the S-N design intercept for studless chain given in DNVGL-OS-E301 [1] ($A_D = 6 \times 10^{10}$, or $\log A_D = 10.778$).

Note that all figures presenting S-N intercepts in the following show $A(\sigma_m, c) = 10^{\log A(\sigma_m, c)}$, as the predicted fatigue life is proportional to the S-N intercept on this scale.

4.2. Base case and effect of partial pooling

Group intercepts for the partial pooling and no-pooling models are presented in Figure 5. The partial pooling model (Figure 5a) clearly constrains the intercepts compared to the unpooled estimates (Figure 5b), which exhibits more pronounced deviations from the average intercept and considerably larger inferential uncertainty. The intraclass correlation of the partial pooling model is $\hat{\rho} = 0.29$ and the ratio of within-group to between-group variances is $\sigma_\epsilon^2/\sigma_\alpha^2 \approx 2.4$, meaning that group-specific information is moderately important. Hence, intercepts for the smallest groups ($n_j = 3$) are approximately halfway between $\hat{\mu}_\alpha$ and the unpooled estimate. For groups with more data, group-specific information is emphasized more than the overall average, increasingly so with increasing group size.

Consider now the intercepts for new chain groups in Figure 5a. There is a distinct clustering of the intercepts for ND and TWI groups, respectively, supporting previous reports on insignificant effects of size (diameter) and material grade for new chain. Both projects include a group of 76 mm R4 chain, so a plausible explanation for deviations between ND and TWI tests may be differences in test setup. One such difference is the number of links included in each test. Recall that ND used 7 links, whereas TWI used 11 links for 76 mm chain and 7 links for 127 mm chain. As the weakest out of 11 links is likely to fail before the weakest out of 7 links, there *could* be a minor size effect that is disguised by a difference in number of links. On the other hand, the deviations could be due to other, unidentified differences related to the execution of the tests by ND and TWI, respectively. In any case, the deviations are small, practically insignificant in this context, and we would be reluctant to conclude based on limited group sizes. Slightly larger variation is observed between the VIC groups, containing tests performed at a range of mean loads. This does not necessarily suggest a difference in the mean load effect for R4 compared to R5 chain, because (i) deviations are still limited, and (ii) the VIC tests were performed for a range of diameters and with a varying number of links.

The groups with used chain generally exhibit a larger between-group variation than for new chain, even for the P1 groups containing samples of the same size and material grade. One group stands out in particular: P6-R3-137, which is the only group with used R3 chain. The group intercept for this group is the one that is shifted the most to the left in Figure 5a, meaning that it is the group that underperforms the most compared to what the model predicts on average. Possible explanations include: (i) It is by chance (this a possible but not a likely explanation); (ii) It is due to larger prior fatigue damage for this group compared to other groups (in this case it is not due to the long service life (18 years) alone, as there are several used chain groups with service life 18-20 years that performed better in the tests); (iii) The corrosion grade scale is not applied consistently for this particular group; (iv) The corrosion effect is different for R3 chain compared to R4 chain. However; until more used R3 chain samples are included or a more objective measure for chain condition may be applied, there is no basis for distinguishing between these possible contributions to the observed deviation. In any case, the intercepts of the two P6 groups, which both include samples with $c = 4$ and were tested at mean loads that are not too different, illustrate that platform is of lesser importance compared to other hidden variables.

Estimated slope coefficients and associated uncertainty across the partial, complete- and no-pooling models are visualized in Figure 6. All three models agree well on the mean load effect (β_1), except for increasing uncertainty as the degree of pooling is reduced. A plausible explanation for the good agreement is that much information about the mean load effect is contained within some few groups with samples tested at both high and low mean loads (cf. Table 3). This is not the case for chain condition, which varies mostly between groups and less within groups, leading to larger deviations in the estimated corrosion grade effect (β_2). The partial pooling estimate appears as a compromise between the complete- and no-pooling estimates, and slightly closer to the complete-pooling model, indicating that it is able to extract information from chain conditions across groups without overfitting the model.

In conclusion, the partial pooling model performs well for the current data set and grouping criterion, with limited risk of overfitting, despite the large number of groups and the small average group size.

4.3. Alternative predictors

Focus is now shifted to the alternative mean load and corrosion grade predictors (models 4 and 5 in Table 4). Compared to the base case, both models perform equally well with regards to standard deviation

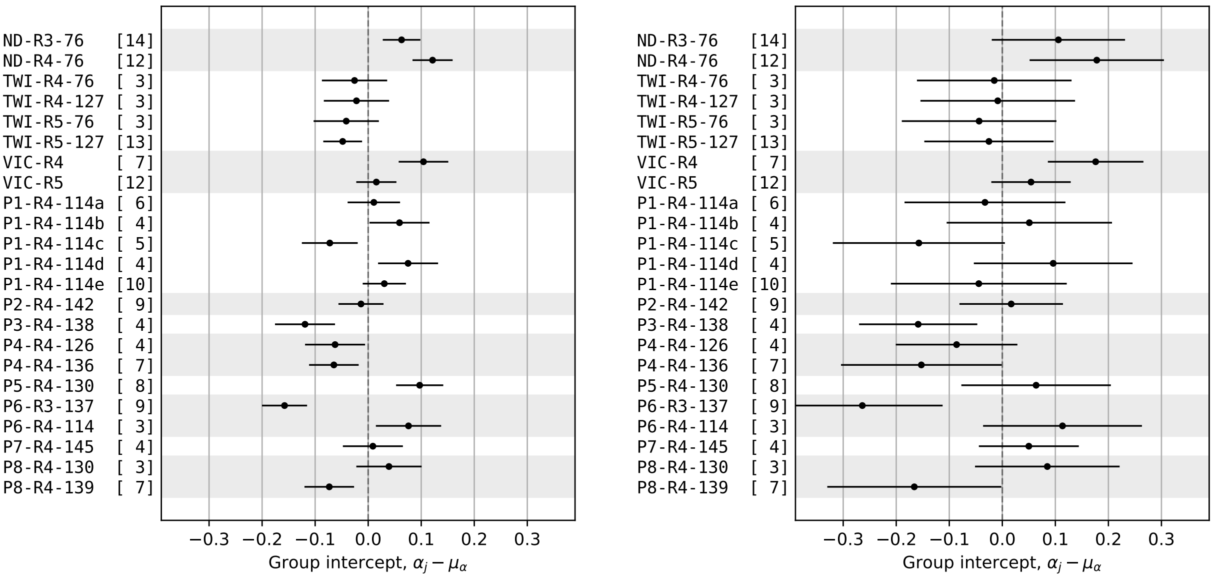

(a) Partial pooling, $\hat{\mu}_\alpha = 12.236$.

(b) No pooling, $\hat{\mu}_\alpha = 12.177$.

Figure 5: Group intercepts for partial pooling and no-pooling models with base case predictors; $g_1(\sigma_m) = \lambda_m$, $g_2(c) = c$. Error bars correspond to standard error of group intercepts, $\hat{\alpha}_j$. Number of tests (n_j) given in brackets. Alternating background shading is used to distinguish between platforms. Note that difference in average intercept (μ_α) between models is not reflected in figure.

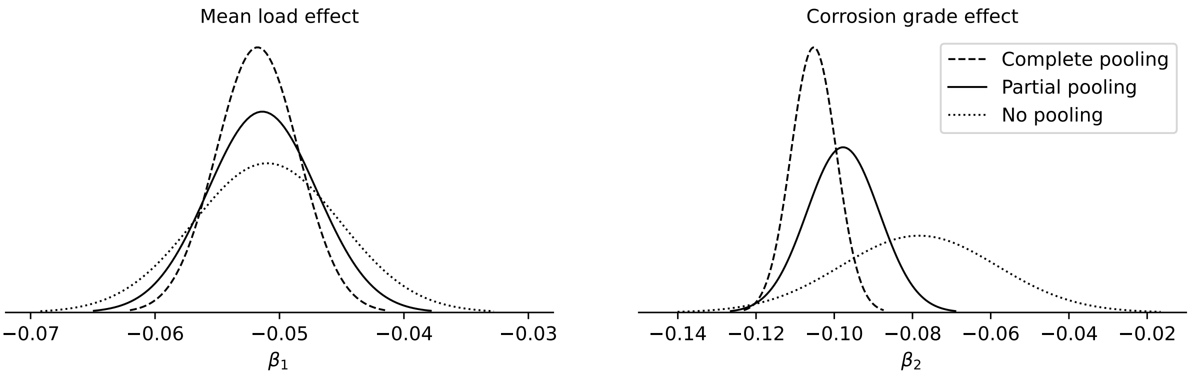

Figure 6: Comparison of slope coefficients estimated from complete-pooling, partial pooling and no-pooling. Probability density function of $\beta \sim N(\hat{\beta}, \mathrm{se}(\hat{\beta})^2)$ where $\hat{\beta}$ is estimated coefficient and se(.) is the standard error. Base case predictors: $g_1(\sigma_m) = \lambda_m$ and $g_2(c) = c$.

of residuals ($\hat{\sigma}_\epsilon$) but estimate a higher group-level error ($\hat{\sigma}_\alpha$). This implies that they are able to describe within-group variations of the data well, but perform slightly worse in describing between-group variations. This results in a larger spread for the group intercepts, shown in Figure 7.

The alternative mean load predictor, $g_1(\sigma_m) = \sigma_m$ [MPa], differs from using λ_m [% MBL] as follows. Consider two samples of the same diameter but of different material grades, that are tested at the same mean load when expressed in percentage of MBL (i.e., same value of λ_m). The sample with the higher material grade is then tested at a higher nominal mean stress (σ_m) due to a higher MBL. Specifically, the nominal mean stress will be around 23% higher for R4 compared to R3 chain, and around 17% higher for R5 compared to R4 chain [28]. In other words; if σ_m were representative as a predictor for the mean load effect, we would expect the lower material grade to perform better than the higher grades when tested at the same mean load level in percentage of MBL.

In practice, by comparison to the base case model with $g_1(\sigma_m) = \lambda_m$ (Figure 5a), the effect of $g_1(\sigma_m) = \sigma_m$ (Figure 7a) is that the intercepts for R3 groups are shifted left compared to R4 groups, and intercepts for R5 groups are shifted right. As a result, the ND and TWI group intercepts now exhibit a distinct spread. Considering that these groups contain fairly homogeneous samples, all but one tested at a mean load of 20% MBL (the one exception being a TWI test at 10% MBL), this larger spread weighs against using nominal mean stress as the mean load predictor. Note also that (i) the one used chain group with R3 chain (P6-R3-137) is shifted left and now deviates even more from the average intercept, and (ii) the intercepts for VIC groups are actually shifted to agree very well for this model. Strictly, the latter observation favors the use of nominal mean stress, but it does not outweigh the larger spread for ND and TWI tests and the overall increase in between-group variation ($\hat{\sigma}_\alpha$).

Two main observations are made by comparison of the model with alternative corrosion grade predictor, $g_2(c) = \log c$, to the base case model. Firstly, it has minor influence on the estimated mean load effect, both in terms of $\hat{\beta}_1$ and its estimated standard error (Table 4). This is consistent with the results discussed in the previous subsection, indicating that much information about the mean load effect is contained within groups with no or limited variation of corrosion grade. Secondly, the between-group variation is only slightly increased, from $\hat{\sigma}_\alpha = 0.092$ to $\hat{\sigma}_\alpha = 0.104$, making it more difficult to observe from visual inspection of group intercepts (Figure 7b, compare to base case in Figure 5a). It is further noted that the estimated S-N intercept at the reference level ($\log A_{\mathrm{ref}}$) is higher for this model, with a fatigue life ratio of 1.06 compared to the base case model. However; the $\log c$ function describes a more rapid degradation of the fatigue capacity when the corrosion grade increases from $c = 1$, as illustrated in Figure 8. The difference is largest around $c = 3$ (Figure 8b), with the base case model roughly 25% on the high side, then diminishes for increasing values of c. Since the model is purely empirical, however, it provides no basis for choosing one function over the other besides the difference in between-group variation.

In conclusion, these results support the base case model over the alternative predictors $g_1(\sigma_m) = \sigma_m$ and $g_2(c) = \log c$. One could argue that the latter option makes a conservative choice for most of the corrosion grade scale, but overall it has less support in the data set.

4.4. New vs. used chain data

Results from applying the partial pooling model for analysis of new chain and used chain data separately are now addressed (models 6 and 7 in Table 4, respectively). From comparison to the base case analysis ($\hat{\beta}_1 = -0.0514, \hat{\beta}_2 = -0.0977, \hat{\sigma}_\epsilon = 0.144, \hat{\sigma}_\alpha = 0.092$), the following initial observations are made. *For new chain data:* there is good agreement on the mean load effect ($\hat{\beta}_1 = -0.0503$), the model error is slightly reduced ($\hat{\sigma}_\epsilon = 0.142$), the between-group variation is reduced ($\hat{\sigma}_\alpha = 0.079$), and the predicted fatigue capacity for the reference mean load is a little less than 10% on the high side ($N_{\mathrm{ratio}} = 1.08$). *For used chain data:* the model estimates a higher mean load effect ($\hat{\beta}_1 = -0.0547$) and a lower corrosion effect ($\hat{\beta}_2 = -0.0893$), the model error is slightly increased ($\hat{\sigma}_\epsilon = 0.146$), the between-group variation is increased ($\hat{\sigma}_\alpha = 0.099$), and the predicted reference fatigue capacity is roughly 15% of the low side ($N_{\mathrm{ratio}} = 0.87$).

The difference in estimated fatigue capacity for new or as new chain ($c = 1$) at mean load $\lambda_m = 20$ [% MBL] is thus around 25%, when predicted based on new chain data compared to used chain data, and the analysis that is based on all data yields a compromise between these. This is visualized in Figure 9,

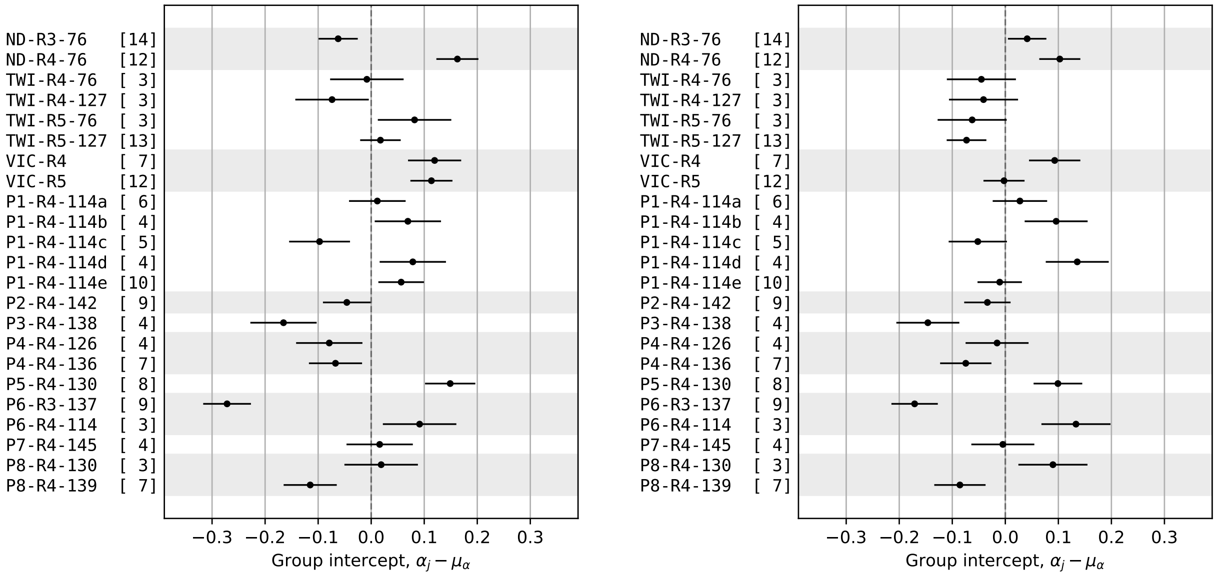

(a) Mean load predictor $g_1(\sigma_m) = \sigma_m$ [MPa] (model 4).

(b) Corrosion grade predictor $g_2(c) = \log c$ (model 5).

Figure 7: Group intercepts for partial pooling model with alternative predictors. See further explanations in caption of Figure 5.

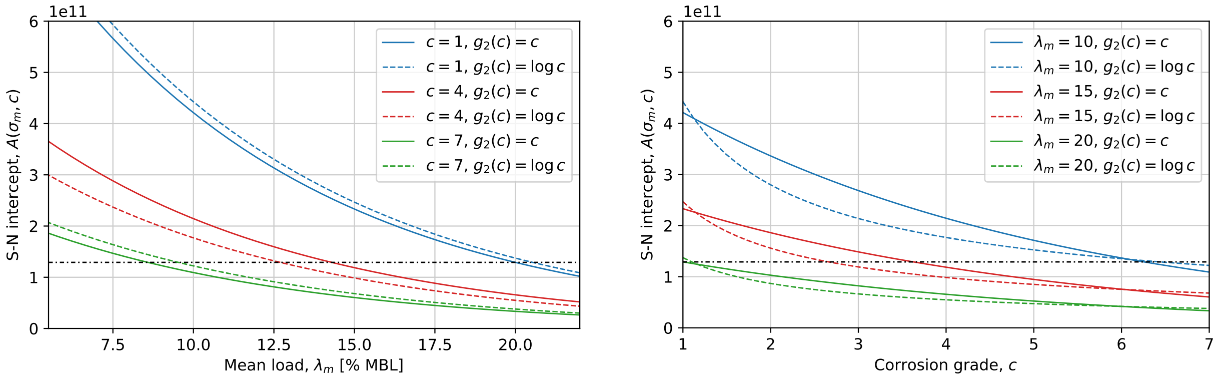

(a) Mean load dependency, for $c \in \{1, 4, 7\}$.

(b) Corrosion grade dependency, for $\lambda_m \in \{10, 15, 20\}$.

Figure 8: S-N intercepts for $g_2(c) = c$ (base case, solid lines) and $g_2(c) = \log c$ (model 5, dashed lines). The horizontal dash-dotted line is located at the reference level $\lambda_m = 20$ [% MBL] and $c = 1$ for the base case model.

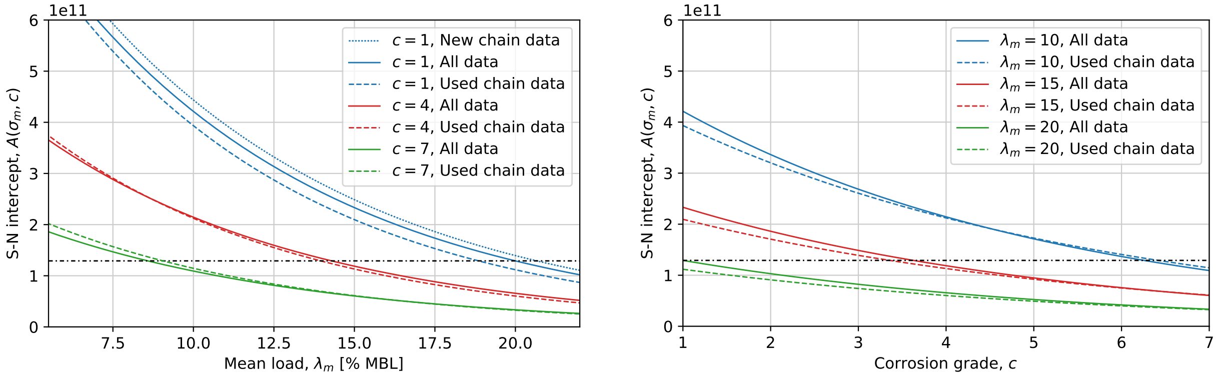

(a) Mean load dependency, for $c \in \{1, 4, 7\}$.

(b) Corrosion grade dependency, for $\lambda_m \in \{10, 15, 20\}$.

Figure 9: S-N intercepts based on different data sets: base case (all data), new chain only and used chain only. The horizontal dash-dotted line is located at the reference level $\lambda_m = 20$ [% MBL] and $c = 1$ for the base case model.

showing S-N intercepts as functions of mean load and corrosion grade. At $c = 1$, the deviations between the curves are fairly consistent across mean loads, although the difference in capacity estimated from new versus used chain data is reduced to around 13% at mean load $\lambda_m = 10$, due to the slightly higher mean load effect for the latter. Since the new chain data contains no information for $c \neq 1$, the S-N intercept based on all data approaches that based on used chain data for increasing corrosion grades. For $c \geq 3$, these curves agree very well (Figure 9b), indicating that the differences in estimated mean load and corrosion effects more or less cancel out.

A possible explanation for the deviations between new and used chain data is that the latter are influenced by prior fatigue loads and damage. This is addressed in the following. The ratio of the allowable fatigue capacity in design to the estimated median capacity is $A_D/A = 10^{-k_n \cdot \hat{\sigma}}$, which for the base case model is around 0.45. In addition, safety factors in the range from 5 to 8 are required on estimated fatigue damage over the service life of the chain [1], reducing the allowable utilization to 6%–9% of the median capacity. Furthermore, the majority of the used chain samples included here were designed to a safety factor of 10 due to stricter company requirements, and retrieved before the end of design life was reached, further reducing the presumed utilization to below 5%. This assessment simplifies the problem somewhat, as there are other factors that influence the *actual* utilization of the chain prior to the fatigue tests:

- Actual fatigue loads that the chains were exposed to during the service life. These may be higher or lower than those estimated in design, depending on the accuracy of the numerical models and computational tools and the amount of conservatism (or, lack of such) included in the design analyses.
- Mean load during operation. A higher or lower mean load during service than in the subsequent test will influence the test result. For samples that were tested at mean loads similar to those experienced during operation, however, this effect should cancel out.
- Chain condition during operation. This will, presumably, have the largest impact on the samples with the lowest corrosion grades. During operation, these will have accumulated loads at a chain condition similar to that in the test. For the samples with the highest corrosion grades, a large share of the fatigue loads will have accumulated for a *better* chain condition than during the test, thereby utilizing less of the fatigue capacity at this chain condition during the prior service life.

Altogether, it seems unlikely that prior fatigue loads alone would be the cause for as much as 25% difference, *on average*, in the fatigue performance of used chain compared to new chain.

Alternative explanations or contributions to the observed differences are the following, possibly in combination. (i) The condition of chains rated to $c = 1$ may not be strictly comparable to that of new chains. For instance, the surface roughness of the used chains may be slightly higher than that which is achieved from pre-soaking new chain samples in artificial seawater. (ii) The mean load and corrosion grade-dependent S-N intercept in (19) with $g_2(c) = c$ implies $A(\sigma_m, c) \propto 10^{\beta_2 \cdot c}$, and this empirical formulation does not likely represent the *true* effect of chain condition. (iii) None of the used chain samples with $c \in \{1, 2\}$ were tested at the highest mean loads (see Figure 3), meaning that prediction of fatigue capacity at the reference level ($\lambda_m = 20, c = 1$) involves extrapolation beyond the used chain data set. With $\lambda_m = 14$, for which several such samples were tested, the difference in estimated capacity is reduced to around 17%.

In any case, the differences between the results obtained for the two data sets are small compared to the estimated mean load and corrosion effects over the range of tested values: they correspond roughly to the effect of increasing the mean load by 2.5 [% MBL] ($10^{\hat{\beta}_1 \cdot 2.5} = 0.74$) or an increase in corrosion grade by one unit ($10^{\hat{\beta}_2 \cdot 1} = 0.80$). Finally, keep in mind that the above discussion is based on the point estimates for the model coefficients. Due to inclusion of fewer fatigue tests, the uncertainties associated with the coefficients are larger when estimated from either new chain or used chain data than for the base case model with all data. The difference in $\hat{\mu}_\alpha$, $\hat{\beta}_1$ and $\hat{\beta}_2$ between the three models is less than or equal to one standard error for each of them.

4.5. Residuals

The residuals, describing differences between the data observed in the tests and those predicted by the model, are given by:

$$r_i = y_i - \hat{y}_i \tag{23}$$

where y_i is the test outcome, defined in (18), and $\hat{y}_i$ is the value predicted by the model. Residuals of the base case model are inspected in Figure 10. They show no clear patterns when plotted versus the predictors (λ_m, c) or the service life of the chain. However; when plotted versus the stress range applied in the test, they reveal a clear trend with positive residuals for high stress ranges. This suggests that the data might favor a *lower* stress range effect (i.e., a lower value of m and a steeper curve in the S-N plot), had it not been fixed at $m = 3$. Figure 1 shows that the tests with highest stress ranges are all for new chain samples. This is consistent with previous studies on the new chain data from ND and TWI: when the stress range effect is estimated from the data, (i) the TWI data results in $m \approx 2.7$ for 127 mm chain and $m \approx 3$ for 76 mm chain [12], and (ii) the ND data results in an even lower stress range effect than that obtained for the TWI data [20].[4]

On the other hand, some used chain studies have suggested that a *higher* stress range effect may be appropriate for highly corroded chain. For the subset P1-R4-114e (cf. Table 1), with $c = 7$, Gabrielsen et al. [11] found that the data indicates $m > 3$ for the tests with $\lambda_m = 18$ [% MBL], and even more so for the tests with $\lambda_m = 8$ [% MBL] (although, with only five tests at each mean load level the uncertainty in estimation of m is large for these two groups). Such trends are not revealed by the residual plots in Figure 10, meaning that they could in principle be disguised by the model as corrosion grade effects or as group differences.

The model issues implied by Figure 10 and the diverging reports for new chain compared to used and highly corroded chain advise caution in how the stress range effect is treated. A step towards better understanding how the model parameters (including m) vary across groups, could be to generalize the varying-intercept model in (5) to a varying-intercept, varying-slope model [22]. However; a complicating factor is that the new chain tests cover a different interval of stress ranges compared to the used chain tests, as shown in Figure 1, such that the resulting experimental design matrix is suboptimal with respect to the spread of stress ranges, mean loads and corrosion grades. Results from a model with even more parameters than the model applied for the present study should therefore be carefully evaluated before any conclusions are drawn, for instance by considering the posterior distributions of the parameters to assess how well defined they are by the data.

4.6. S-N data transformed to reference level

Consider a sample that failed after N_1 cycles in a test associated with the parameters $\{\sigma_{m,1}, c_1\}$, and that we want to predict what the fatigue life would have been had the test been conducted with the same

[4] The steeper curve for the ND data may also be seen from Figure 4 in [12] or Figure 21 in [11].

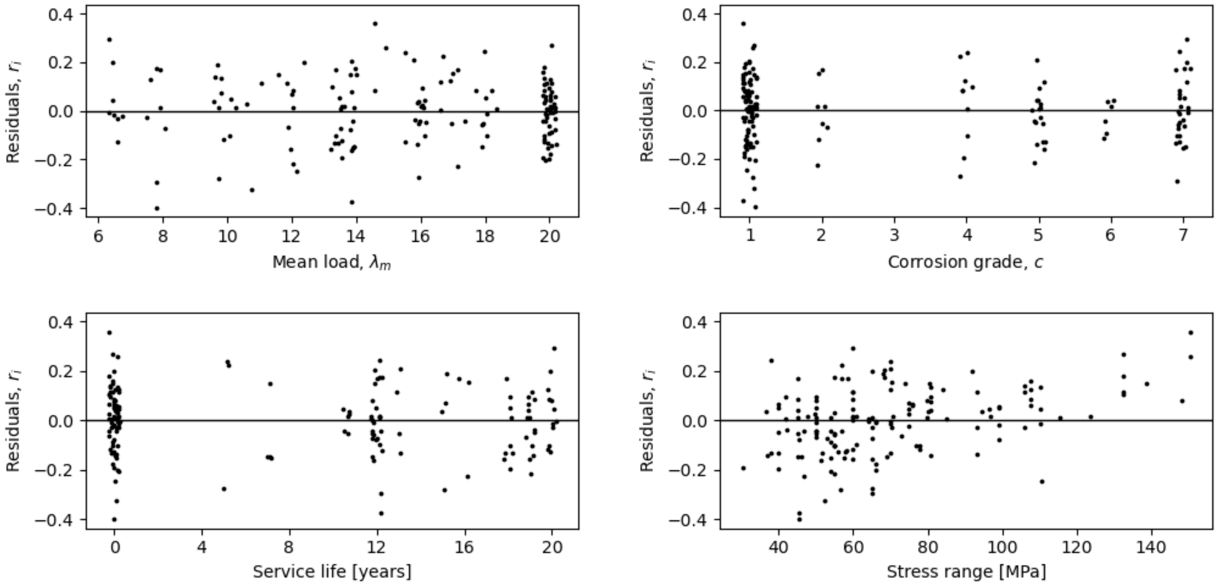

Figure 10: Residual plots for base case. Plotting position has been jittered along horizontal axis for mean load, corrosion grade and service life.

stress range but for a different mean load and corrosion grade, $\{\sigma_{m,2}, c_2\}$. By requiring that $S_2 = S_1$, the resulting transformation obtained from the S-N relation in (1) is simply the ratio of the S-N intercepts for the two states, $A(\sigma_{m,2}, c_2)/A(\sigma_{m,1}, c_1)$. For the base case model it is:

$$\frac{N_2}{N_1} = \underbrace{10^{\beta_1(\lambda_{m,2}-\lambda_{m,1})}}_{\text{Mean load correction}} \cdot \underbrace{10^{\beta_2(c_2-c_1)}}_{\text{Corrosion grade correction}} \tag{24}$$

where N_2 is the predicted fatigue life of the given sample in a test associated with the alternative state, $\{\sigma_{m,2}, c_2\}$. As noted, the transformation has been split into two factors to distinguish between the correction due to differences in mean load and corrosion grade, respectively.

Figure 11 shows a S-N plot with all data transformed by (24) to represent the reference level, $\lambda_m = 20$ [% MBL] and $c = 1$. The scatter of the data, in terms of deviation from the S-N curve, is considerably reduced for both new and used chain tests compared to that seen for the raw data in Figure 1. It is emphasized that the estimated group-specific intercepts, $\hat{\alpha}_j$, are *not* utilized for adjustment of the data for this plot. The between-group variability is instead accounted for by using the total standard deviation, $\hat{\sigma}$, to establish the design curve in accordance with (20). It is noted that two of the used chain samples fall below the design curve of the base case model, which is based on all data (Figure 11a). The fact that these two least favorable results are both for used chain may be due to the larger variability for these data, or it could be that the corrosion grades assigned to them do not fully represent the condition of these samples. In any case, two samples falling below the design curve is acceptable, in principle, considering the total number of tests ($n = 154$) and the required 97.7% exceedance probability. A possible remedy could however be to utilize the model which is based on used chain data only (model 7, cf. Table 4). For this model, the lower estimated mean curve and the higher standard deviation ($\hat{\sigma}$) shifts the design curve just enough towards lower fatigue life for all the samples to fall above the design curve (Figure 11b).

4.7. On assumptions and limitations

We now summarize some of the main findings and conclusions from the previous subsections, and discuss assumptions and limitations that have not yet been addressed.

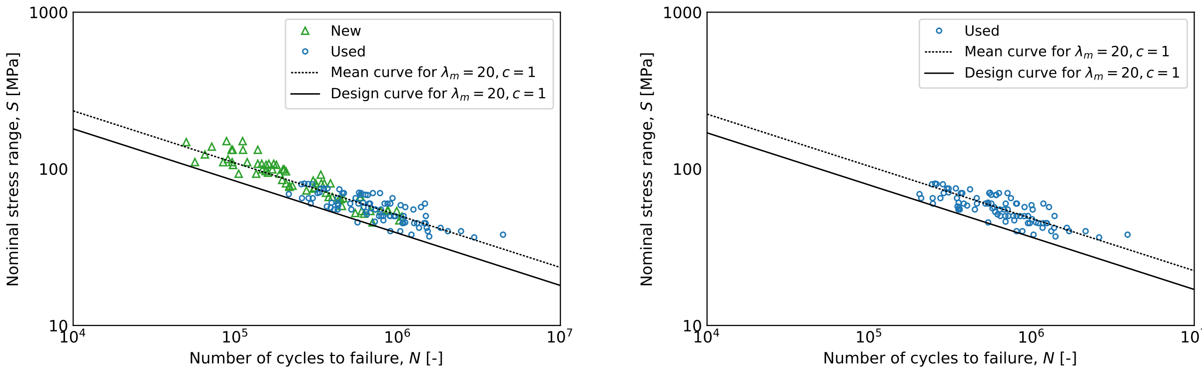

(a) All data, base case model.

(b) Used chain, model based on used chain only (model 7).

Figure 11: S-N data from fatigue tests with number of cycles to failure (N) transformed to represent $\lambda_m = 20$ [% MBL] and $c = 1$.

Grouping criterion and predictors. The hierarchical model is defined with "batch" as the grouping criterion, to limit the adverse influence from hidden variables. This choice leads to a large number of groups and less than seven tests per group on average. Despite the intuitive risk of overfitting, the partial pooling model reassuringly results in a compromise between the alternative complete-pooling or no-pooling models, and slightly closer to the complete-pooling model (cf. Table 4 and Figure 6). Compared to the base case predictors (Section 4.2), alternative mean load and corrosion grade predictors (Section 4.3) perform equally well in terms of describing within-group variability (σ_ϵ), but are to a lesser degree able to describe between-group variations (i.e., larger σ_α). On this basis, the base case model with partial pooling, mean load predictor $g_1(\sigma_m) = \lambda_m$ [% MBL] and corrosion grade predictor $g_2(c) = c$, is adopted as the most adequate.

Used chain data. The model that is based on used chain data only results in a larger within-group variability (σ_ϵ) compared to the model which uses only new chain data (cf. Table 4). This could suggest that corrosion increases the variability of the fatigue performance, although, the differences are small and a systematic study of the variability within groups with different corrosion grades is needed to conclude with confidence. A more pronounced increase is seen for the between-group variability (σ_α), suggesting a larger influence from hidden variables for used chain compared to new chain or that the corrosion grade scale has not been applied consistently across groups. Nevertheless, the deviation observed for the only group with used R3 chain (Figure 5a) indicates that the used chain data with mostly R4 chain could be too homogeneous, such that σ_α might be underestimated. This concern could be addressed by inclusion of more used chain samples, with material grades other than R4.

Chain condition. The corrosion grades assigned to the used chain samples are treated by the regression model as *certain* values. Consequently, the uncertainty that arises from using this subjective measure is not quantified by the model. Until a more objective method for quantification of chain condition is available, the uncertainty in the estimated mean load effect ($\hat{\beta}_2$) therefore cannot be accurately quantified. Moreover, by using nominal stress ranges (i.e., not accounting for loss of cross section) we have assumed that the effect of corrosion is fully represented by the corrosion grade. The potential need to account for material loss for heavily corroded chain has not been addressed. It is also emphasized that the used chain samples have been visually inspected before the tests, to ensure the absence of visible fatigue cracks. Hence, the model is strictly valid only for chain segments subjected to inspections that are at least as accurate as those conducted prior to the tests.

Mean load effect. Tests have been conducted for mean loads in the range from 6% to 20% MBL, with the majority (143 out of 154 tests) from 8% MBL and upwards. It may thus be advisable to apply a cut-off somewhere between 6% and 8% MBL, below which the beneficial effect of a further reduction of the mean load is not taken into account in the mooring chain fatigue assessment. Also, the model should be used cautiously for mean loads above 20% MBL, as the data set includes no tests that can be used to quantify the fatigue performance at higher mean loads.

Slope coefficients and possible interaction effects. By assuming common slope coefficients across groups, the effects they describe are averaged over the data set. Reassuringly, the mean load effect (β_1) estimated for new and used chain, respectively, agree reasonably well. For the effect of corrosion, a common β_2 coefficient is a necessary assumption to provide meaningful estimates, considering the limited variation of the corrosion grade within groups. A more disturbing observation is the potential model issue introduced by assuming a fixed stress range effect ($m = 3$), as revealed by the residual plots (Figure 10). Considering the reports from previous studies regarding seemingly opposite influence on m for new chain compared to highly corroded chain, and also possible influence from the mean load level, future studies might consider to (i) allow m to vary between groups or (ii) include interaction terms quantifying the joint effect of stress range, mean load and corrosion grade. In doing so, the adverse effect of a suboptimal experimental design matrix, with higher stress ranges applied on average for the new chain tests compared to used chain tests, should be carefully assessed.

Design curve. S-N design intercepts presented here are estimated by applying an offset to $\hat{\mu}_\alpha$. This simplification neglects the inferential uncertainty of the slope coefficients which could, in principle, affect the required design curve offset differently at various mean load and corrosion grade levels. A formally more correct approach would be to establish the design curve through for instance Monte Carlo simulation, including inferential uncertainty, to estimate the intercept with 97.72% exceedance probability for a range of mean loads and corrosion grades.

Number of links. We have assumed that the test results represent single link failures, while in practice, they represent failure of the weakest out of multiple links. This has the following impact on the results: (i) the estimated distribution is shifted towards lower fatigue capacity, (ii) the within-group variability (σ_ϵ) is underestimated, and (iii) the assumption of normal distributed errors is questionable. The former two effects have opposite effects in terms of conservatism, and they are all strengthened by considering first fractures only. In sum, however, the assumption is conservative. Note also that differences in number of links applied in the tests lead to inconsistencies across groups. This is not addressed, but may in principle be perceived by the model as a group effect. For an example of the fatigue capacity of the weakest link in a chain segment compared to that of a single link, see Section 5.2.

Concluding remark. The model and the results from this study provide important input to better understanding the fatigue capacity of mooring chain, in particular with respect to the effects of mean load and chain condition. However, more research is needed to provide answers to the questions raised herein.

5. Impact on fatigue capacity and reliability

The impact of the results from the present work is now presented. The fatigue capacity is addressed first, by comparison to S-N intercepts published previously. The effect of within-group correlation on the capacity of the weakest link within a chain segment is presented thereafter. In this Section, all results from the present work are for the base case model.

5.1. Fatigue capacity

The fatigue capacity predicted by the base case model is now compared to two S-N models published previously. Note that for consistency, *design* curves are compared. This also enables comparison to the design curve from DNVGL-OS-E301 [1].

Fernandez et al. [13] considered new chain samples tested at mean loads ranging from 7%–17%. A total of 24 tests were considered, including the VIC tests listed in Table 1. They applied the Smith-Watson-Topper

(SWT) mean load correction model, and transformed the stress ranges applied in the tests to represent different mean load levels. A S-N intercept was then fitted to the data at each level, with the stress range effect fixed at $m = 3$. The mean load dependency was then established by fitting a fourth-order polynomial to these S-N intercepts, and the resulting design curve intercept was expressed as

$$A_D(\lambda_m) = 6.989\times10^{11} - 7.435\times10^{10}\cdot\lambda_m + 3.174\times10^{9}\cdot\lambda_m^2 - 6.173\times10^{7}\cdot\lambda_m^3 + 4.521\times10^{7}\cdot\lambda_m^4 \quad (25)$$

Lone et al. [18] considered a complete pooling model and the test data in Table 1, excluding the VIC tests and the batch P1-R4-114e. In Table 5, the resulting design curve parameters are listed along with those from the base case model of the present study.

Figure 12 presents the S-N intercepts for a range of mean load and corrosion grade levels. Consider first the model by Fernandez et al. in Figure 12a. Since it was based on new chain data, it is comparable to the base case model for $c = 1$. They agree reasonably well for mean loads in the range 15%–20% MBL. The difference between them increases for lower mean loads, with the base case model on the low side. This deviation could be partly due to the simpler formulation used to describe the mean load dependency for the present study (i.e., $A \propto 10^{\beta_1\cdot\lambda_m}$ vs. a polynomial of fourth order), and partly due to differences between the mean load effect estimated empirically and that which results from the SWT transformation.

The base case model is now compared to the model from [18]. They are seen to agree well across the mean loads and corrosion grades considered, with the largest differences observed for mean loads below 10% MBL. In any case, these minor deviations are of little practical importance.

Finally, it is noted that all three models agree well with the design curve intercept from [1] for the reference level ($\lambda_m = 20, c = 1$).

Table 5: S-N design curve parameters: base case model vs. Lone et al. [18]. Predictors are $g_1(\sigma_m) = \lambda_m$ and $g_2(c) = c$ for both models.

Model	m	$\hat{\mu}_{\alpha,D}$	$\hat{\beta}_1$	$\hat{\beta}_2$
Present study, base case model	3	11.891	-0.0514	-0.0977
Lone et al. [18]	3	11.904	-0.0507	-0.1062

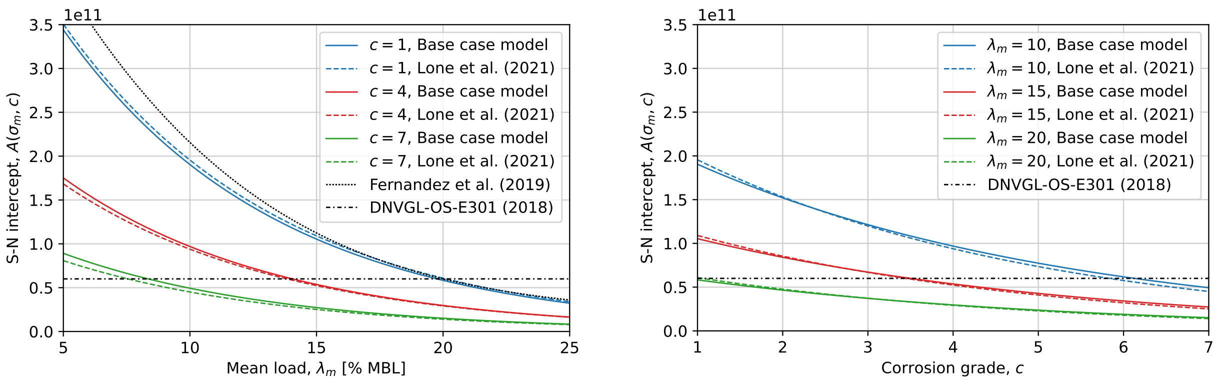

(a) Mean load dependency, for $c \in \{1, 4, 7\}$.

(b) Corrosion grade dependency, for $\lambda_m \in \{10, 15, 20\}$.

Figure 12: Comparison of S-N design intercepts. Fernandez et al. (2019) refers to [13] and Lone et al. (2021) refers to [18]. S-N intercept from DNVGL-OS-E301 [1] is included for reference.

5.2. *Influence of within-segment correlation*

The hierarchical model accounts for, and quantifies, correlation between the fatigue capacity of chain links within a group. The effect of this correlation on the fatigue capacity distribution for the weakest link within a chain segment, and subsequently, for the fatigue reliability, is now addressed. Note that a premise for this part is that we consider a segment for which the group-specific intercept, α_j, is unknown.

5.2.1. *Weakest link resistance*

We consider a chain segment composed of n identical chain links, and assume that the links are exposed to the same mean load and associated with the same corrosion grade. The S-N intercept for each link is then

$$\log A_i(\lambda_m, c) = \mu_\alpha + \beta_1 \cdot \lambda_m + \beta_2 \cdot c + \eta + \epsilon_i \tag{26}$$

where $i \in (1, \ldots, n)$ is an index for links, $\eta \sim N(0, \sigma_\alpha^2)$ represents segment-level variability and $\epsilon \sim N(0, \sigma_\epsilon^2 \boldsymbol{I})$ represents between-link variability. Note that an equivalent representation is to replace η and ϵ_i by $\epsilon_i^{\text{all}} = \eta + \epsilon_i$, with $\epsilon^{\text{all}} \sim N(\mathbf{0}, \mathbf{\Sigma})$. Here, $\mathbf{\Sigma}$ is a $n \times n$ covariance matrix with $\sigma^2 = \sigma_\alpha^2 + \sigma_\epsilon^2$ on the diagonal and σ_α^2 elsewhere [22]. This implies that $\rho = \sigma_\alpha^2/\sigma^2$, the intraclass correlation defined in (13), quantifies the correlation between links in the segment under the model in (26).

The fatigue capacity of the weakest link within the segment may now be expressed as

$$A_W(\lambda_m, c) = \min_{i=1}^{n}\{10^{\epsilon_i}\} \cdot 10^{\eta} \cdot 10^{\mu_\alpha + \beta_1 \cdot \lambda_m + \beta_2 \cdot c} \tag{27}$$

where subscript $\cdot_W$ refers to "weakest". For convenience, we define:

$$W := \min_{i=1}^{n}\{10^{\epsilon_i}\} \tag{28}$$

$$W' := W \cdot 10^{\eta} \tag{29}$$

This implies that W is the minimum of n lognormal variables, for which the exact distribution may be obtained from order statistics [29]. See [30] for a detailed example. The factor W' is the ratio of the weakest link's fatigue capacity to the median capacity at the given mean load and corrosion grade level, and may thus be interpreted as a normalized measure for the weakest link resistance.

Figure 13 shows the probability density function of W' for three segment sizes, $n \in \{20, 100, 500\}$, for the following two cases:

- Correlated links: $\sigma_\epsilon = 0.144$ and $\sigma_\alpha = 0.092$, which implies $\rho = 0.29$. This corresponds to the base case model, see Table 4. The distribution of W' is generated by Monte-Carlo simulation with sample size 5×10^5, and presented as normalized histograms.
- Independent links: $\sigma_\epsilon = 0.171$ and $\sigma_\alpha = 0$, i.e., $\rho = 0$. The distribution of W' is modeled as an exact extreme minimum distribution.

Compared to independent links, the case with correlated links yields wider distributions with the mode shifted towards right. The implication is that the weakest out of n correlated links is likely to deviate less from the median capacity compared to the weakest out of n independent links. However, it is also seen that for a given segment size, the distributions are not too different in the lower left tail which is important for the fatigue reliability. This is addressed next.

5.2.2. *Fatigue reliability*

A reliability formulation for mooring chain fatigue including the effects of mean load and degradation due to corrosion is presented in [30], based on a S-N model consistent with that applied herein. Using this formulation, we will now assess the influence of the estimated between-link correlation on the fatigue failure probability.

The probability of fatigue failure after N_y years of a chain segment with n links may be expressed as

$$p_f = \mathrm{P}\left[\, g(\boldsymbol{X}; N_y, n) \leq 0 \,\right] \tag{30}$$

where $g(\boldsymbol{X}; N_y, n)$ is the limit state function, defined as:

$$g(\boldsymbol{X}; N_y, n) = D_{\text{cr}} - D_W(\boldsymbol{X}; N_y, n) \tag{31}$$

Here, D_{cr} is the critical fatigue damage (i.e., the fatigue damage at failure), and $D_W(\boldsymbol{X}; N_y, n)$ is the fatigue damage of the weakest link:

$$D_W(\boldsymbol{X}; N_y, n) = \frac{1}{W \cdot 10^{\eta}} \sum_{k=1}^{N_y} \frac{Q_s^m \cdot Z_k}{10^{(\mu_\alpha + \beta_1 \cdot Q_m \cdot \lambda_m + \beta_2 \cdot C_k)}} \tag{32}$$

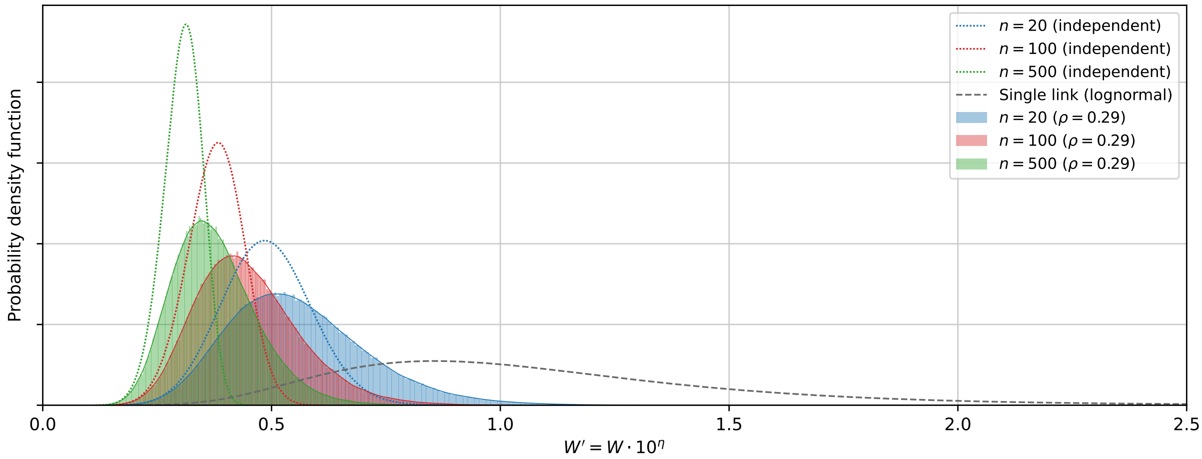

Figure 13: Probability density function of $W' = W \cdot 10^{\eta}$ for chain segment with n links. Independent ($\rho = 0$) vs. correlated ($\rho = 0.29$) links. Solid lines are kernel density estimates for the normalized histograms, and are included for visualization.

where k is an index for year; W is defined in (28) and η represents the segment-level variability as discussed in relation to (26); C_k is the corrosion grade of the chain in the k^{th} year, assumed to increase linearly from 1 at installation to its value at the end of the service life, denoted C_{end}. The remaining variables of this expression are described in Table 6, along with distributions used to model them. For further details, see [30].

Note that by modeling the S-N coefficients $(\mu_\alpha, \beta_1, \beta_2)$ as fixed variables, the inferential uncertainty (related to the standard errors of the coefficients) is neglected. However, for the model applied in [30], this uncertainty was shown to be of negligible importance for the fatigue damage.

Figure 14 shows the annual probability of failure for the last ten years of an assumed service life of 15 years, estimated by importance sampling with sample size 5×10^4. Correlation between links has the largest impact for the largest segment size ($n = 500$). For this segment, the failure probability is higher by a factor of around 1.7 for the case with independent links compared to correlated links with $\rho = 0.29$. This effect is less than the change in failure probability from one year to the next, or the effect of considering a shorter chain segment. In any case, this difference is small, considering that reliability calculations are concerned with orders of magnitude rather than exact numbers. Hence, for the reliability model considered here, the between-link correlation is of limited importance.

6. Conclusions

Full scale fatigue test data of new and used studless mooring chain have been considered. Both new chain data and used chain data include tests conducted at a range of mean load levels between 6% and 20% MBL. In addition, the used chain samples represented a range of chain conditions, quantified by means of a custom corrosion grade scale ranging from 1 (new or as new chain) to 7 (heavily corroded chain). Based on an extended S-N formulation with a parameterized S-N intercept parameter, the effects of mean loads and corrosion grade were quantified empirically from the data. A hierarchical varying-intercept model was used for the regression analysis, to properly account for and quantify correlations within subsets of the data.

The results show that mean load and chain condition have a significant impact on the fatigue performance of the chains, such that the fatigue life (i) increases when the mean load is reduced and (ii) decreases when the corrosion grade increases. Over the range of mean loads and corrosion grades considered, these effects are considerably larger than the differences in estimated fatigue life for new versus used chain when evaluated at the same mean load and corrosion level.

Table 6: Variables for case study of influence on fatigue failure probability from correlation between links in the chain segment.

Variable	Symbol	Unit	Dimension[a]	Distributed as	Mean	St.dev.	CoV[b]
Fatigue damage at failure	D_{cr}	–	1	$LN(0, 0.29)$	1.04	0.31	0.30
Annual fatigue load	Z_k	MPa^3	N_y	$LN(19.96, 0.39)$	5×10^8	2×10^8	0.40
Representative mean load	λ_m	% MBL	1	Fixed	15.0	–	0.04
Corrosion grade at end of service life	C_{end}	–	1	$U(1, 7)$	4	1.7	–
Model uncertainty (stress ranges)	Q_s	–	1	$N(1.0, 0.10^2)$	1.0	0.10	0.10
Model uncertainty (mean loads)	Q_m	–	1	$N(1.0, 0.10^2)$	1.0	0.10	0.10
S-N model[c]							
Constant term	μ_α	–	1	Fixed	12.236	–	–
Mean load effect	β_1	–	1	Fixed	−0.0514	–	–
Corrosion grade effect	β_2	–	1	Fixed	−0.0977	–	–
Stress range effect	m	–	1	Fixed	3	–	–
Model error[d]	σ	–	1	Fixed	0.171	–	–

St.dev.: standard deviation. CoV: coefficient of variation.
[a] Number of i.i.d. random variables with this distribution.
[b] CoV is given when used to define the distribution.
[c] Base case model, cf. Table 4.
[d] Total standard error of model, see Equation (17).

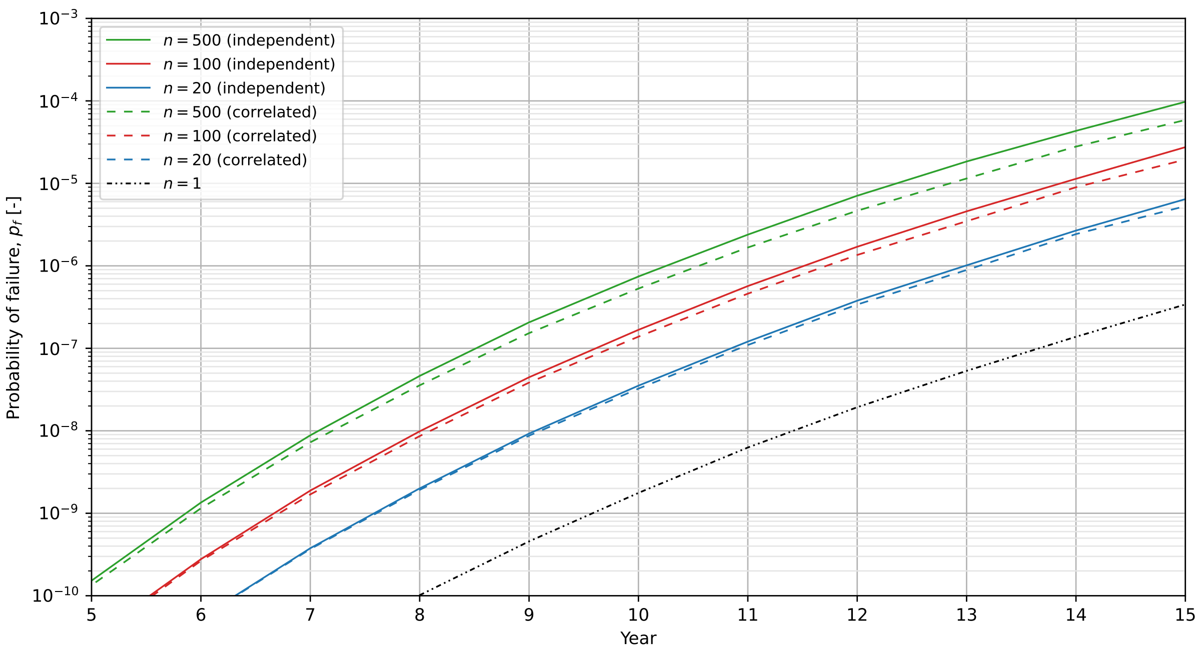

Figure 14: Annual probability of failure for the last 10 years of operation for a chain segment with n links. Independent ($\rho = 0$) vs. correlated ($\rho = 0.29$) fatigue capacity between links in the segment.

For chain links within a group, the model estimates that the fatigue capacity is moderately correlated. A case study on the influence of this between-link correlation has been presented. Compared to assuming independent fatigue capacity for links within a chain segment it was demonstrated that the estimated correlation (i) shifts the distribution of the weakest link capacity towards higher fatigue capacity and makes it wider, but (ii) has limited importance for the probability of fatigue failure.

Further work. The present work has been limited to assuming (i) fixed stress range effect ($m = 3$) and (ii) common slope coefficients across groups for the effects of mean load and chain condition. Validation of the model indicates that the former assumption is questionable, and should be further assessed for future work. Methods to measure objectively the chain condition would greatly improve the model, and mitigate uncertainties that cannot be accurately quantified based on the current data. Furthermore, the used chain data are all of R4 material grade expect one group of R3 chain. The results have suggested that the homogeneous used chain data may lead to an underestimation of the variability of the fatigue capacity. Inclusion of more used chain tests for material grades other than R4 would serve to further quantify this. Finally, fatigue tests of both new and used chains at mean loads above 20% MBL would contribute to an improved understanding and quantification of the mean load effect for high mean loads. This would be of relevance for the mooring systems of for instance floating wind turbines, possibly operating at such higher mean loads.

Acknowledgment

This study was financed by the Research Council of Norway, through the project 280705 “Improved lifetime estimation of mooring chains” (LIFEMOOR). TWI is acknowledged for providing test results from the TWI JIP on fatigue performance of mooring chain. Vicinay is acknowledged for sharing results from the new chain tests performed at a range of mean load levels.

Nomenclature

$\log(\cdot)$	Common logarithm
$\mathrm{se}(\cdot)$	Standard error
$\sim$	distributed as
$p(\cdot)$	Probability density
$LN(\mu, \sigma)$	Lognormal distribution with scale parameter $\exp\{\mu\}$ and shape parameter σ
$N(\mu, \sigma^2)$	Normal distribution with mean μ and variance σ^2
$U(a, b)$	Uniform distribution with support $[a, b]$
α_j	Group-specific intercept, for $j \in \{1, \dots, J\}$, see (5)
β_1	Mean load effect coefficients, see (3)
β_2	Corrosion grade effect coefficients, see (3)
$\boldsymbol{\beta}$	Vector of regression coefficients
ϵ	Data-level regression error, see (5)
η	Group-level regression error, see (6)
λ_m	Mean load [% MBL]

μ_α	Mean intercept, see (5)
σ	Total standard deviation, see (17)
σ_m	Mean stress [MPa]
σ_α	Group-level standard error, see (4)
σ_ϵ	Data-level standard error, see (4)
$A(\sigma_m, c)$	Mean load and corrosion dependent intercept parameter of S-N curve, see (19)
$A_D(\sigma_m, c)$	Mean load and corrosion dependent design intercept parameter of S-N curve, see (20)
c	Corrosion grade, support $[1, 7]$
$g_1(\sigma_m)$	Mean load function, see (19)
$g_2(c)$	Corrosion grade function, see (19)
m	Slope parameter of S-N curve
N	Number of cycles to failure, see (1)
S	Stress range [MPa]
CoV	Coefficient of Variation
i.i.d.	independent and identically distributed
MBL	Minimum Breaking Load

References

[1] DNV GL, Offshore Standard - Position mooring (DNVGL-OS-E301), Edition July 2018 (2018).

[2] API, Design and Analysis of Stationkeeping Systems for Floating Structures (API RP 2SK), Third Edition (incl. 2008 Addendum) (2008).

[3] ISO 19901-7, Petroleum and natural gas industries - Specific requirements for offshore structures - Part 7: Stationkeeping systems for floating offshore structures and mobile offshore units (2013).

[4] C. R. A. Schneider, S. J. Maddox, Best practice guide on statistical analysis of fatigue data, Doc. IIW-XIII-WG1-114 - 03, International Institue of Welding (IIW) (2003).

[5] Ø. Gabrielsen, K. Larsen, O. Dalane, H. B. Lie, S.-A. Reinholdtsen, Mean Load Impact on Mooring Chain Fatigue Capacity: Lessons Learned From Full Scale Fatigue Testing of Used Chains, in: Proceedings of the ASME 2019 38th International Conference on Ocean, Offshore and Arctic Engineering, no. OMAE2019-95083, 2019. doi:https://doi.org/10.1115/OMAE2019-95083.

[6] S. Fredheim, S.-A. Reinholdtsen, L. Håskoll, H. B. Lie, Corrosion Fatigue Testing of Used, Studless, Offshore Mooring Chain, in: Proceedings of the ASME 2013 32nd International Conference on Ocean, Offshore and Arctic Engineering, no. OMAE2013-10609, 2013.

[7] Ø. Gabrielsen, K. Larsen, S. A. Reinholdtsen, Fatigue testing of used mooring chain, in: Proceedings of the ASME 2017 36th International Conference on Ocean, Offshore and Arctic Engineering, no. OMAE2017-61382, 2017. doi:10.1115/OMAE2017-61382.

[8] Ø. Gabrielsen, T. Liengen, S. Molid, Microbiologically Influenced Corrosion on Seabed Chain in the North Sea, in: Proceedings of the ASME 2018 37th International Conference on Ocean, Offshore and Arctic Engineering, Vol. 3, 2018, pp. 1–9. doi:10.1115/OMAE2018-77460.
URL https://doi.org/10.1115/OMAE2018-77460

[9] K.-t. Ma, Ø. Gabrielsen, Z. Li, D. Baker, A. Yao, P. Vargas, M. Luo, A. Izadparast, A. Arredondo, L. Zhu, N. Sverdlova, I. S. Høgsæt, Fatigue Tests on Corroded Mooring Chains Retrieved From Various Fields in Offshore West Africa and the North Sea, in: Proceedings of the ASME 2019 38th International Conference on Ocean, Offshore and Arctic Engineering, no. OMAE2019-95618, 2019.

[10] Ø. Gabrielsen, I. Kulbotten, I. Perez, L. Haskoll, Inner Bend Cracks in Mooring Chain : Investigation of Cracks, in: Proceedings of the ASME 2019 38th International Conference on Ocean, Offshore and Arctic Engineering, no. OMAE2019-95084, 2019.

[11] Ø. Gabrielsen, S.-A. Reinholdtsen, B. Skallerud, P. J. Haagensen, M. Andersen, P.-A. Kane, Fatigue Capacity of Used Mooring Chain - Results from Full Scale Fatigue Testing at Different Mean Loads, in: Proceedings of the ASME 2022 41st International Conference on Ocean, Offshore and Arctic Engineering, no. OMAE2022-79649, Hamburg, Germany, 2022.
[12] Y. Zhang, P. Smedley, Fatigue Performance of High Strength and Large Diameter Mooring Chain in Seawater, in: Proceedings of the ASME 2019 38th International Conference on Ocean, Offshore and Arctic Engineering, no. OMAE2019-95984, 2019. doi:10.1115/OMAE2019-95984.
[13] J. Fernández, A. Arredondo, W. Storesund, J. J. González, Influence of the Mean Load on the Fatigue Performance of Mooring Chains, in: Proceedings of the Annual Offshore Technology Conference, no. OTC-29621-MS, 2019. doi:10.4043/29621-MS.
[14] I. Martinez Perez, P. Bastid, A. Constantinescu, V. Venugopal, Multiaxial Fatigue Analysis of Mooring Chain Links Under Tension Loading: Influence of Mean Load and Simplified Assessment, in: Proceedings of the ASME 2018 37th International Conference on Ocean, Offshore and Arctic Engineering, Vol. 3, 2018, pp. 1–11. doi:10.1115/OMAE2018-77552.
URL https://doi.org/10.1115/OMAE2018-77552
[15] I. Martinez Perez, A. Constantinescu, P. Bastid, Y. H. Zhang, V. Venugopal, Computational fatigue assessment of mooring chains under tension loading, Engineering Failure Analysis 106 (June) (2019) 104043. doi:10.1016/j.engfailanal.2019.06.073.
URL https://doi.org/10.1016/j.engfailanal.2019.06.073
[16] N. Dowling, S. Thangjitham, An Overview and Discussion of Basic Methodology for Fatigue, Fatigue and Fracture Mechanics: 31st Volume (2000) 3–36doi:10.1520/stp14791s.
[17] N. E. Dowling, Mean Stress Effects in Stress-Life and Strain-Life Fatigue, in: SAE Technical Papers, Vol. 2, SAE International, 2004. doi:10.4271/2004-01-2227.
URL https://www.sae.org/content/2004-01-2227/https://doi.org/10.4271/2004-01-2227
[18] E. N. Lone, T. Sauder, K. Larsen, B. J. Leira, Fatigue assessment of mooring chain considering the effects of mean load and corrosion, in: Proceedings of the ASME 2021 40th International Conference on Ocean, Offshore and Arctic Engineering, no. OMAE2021-62775, Virtual, 2021. doi:10.1115/OMAE2021-62775.
[19] J. Mendoza, P. J. Haagensen, J. Köhler, Analysis of fatigue test data of retrieved mooring chain links subject to pitting corrosion, Marine Structures 81 (2022) 103119. doi:10.1016/j.marstruc.2021.103119.
URL https://linkinghub.elsevier.com/retrieve/pii/S0951833921001702
[20] Noble Denton, Corrosion Fatigue Testing of 76mm Grade R3 & R4 Studless Mooring Chain, Joint Industry Study Report H5787/NDAI/MJV, Rev.0 (2002).
[21] J. Fernández, W. Storesund, J. Navas, Fatigue performance of grade R4 and R5 mooring chains in seawater, in: Proceedings of the ASME 2014 33rd International Conference on Ocean, Offshore and Arctic Engineering, no. OMAE2014-23491, 2014. doi:10.1115/OMAE2014-23491.
[22] A. Gelman, J. Hill, Data Analysis Using Regression and Multilevel/Hierarchical Models, Analytical methods for social research, Cambridge University Press, Cambridge, 2007. doi:10.1017/CBO9780511790942.
[23] M. J. Lindstrom, D. M. Bates, Newton—Raphson and EM Algorithms for Linear Mixed-Effects Models for Repeated-Measures Data, Journal of the American Statistical Association 83 (404) (1988) 1014–1022. doi:10.1080/01621459.1988.10478693.
URL http://www.tandfonline.com/doi/abs/10.1080/01621459.1988.10478693
[24] A. Gelman, J. Carlin, H. Stern, D. B. Dunson, A. Vehtari, D. B. Rubin, Bayesian Data Analysis, 3rd Edition, Texts in statistical science, CRC Press, Boca Raton, Fl, 2014.
[25] J. K. Kruschke, Doing Bayesian Data Analysis, 2nd Edition, Academic Press, 2015. doi:10.1016/B978-0-12-405888-0.00001-5.
URL https://linkinghub.elsevier.com/retrieve/pii/B9780124058880099992
[26] S. Seabold, J. Perktold, Statsmodels: Econometric and Statistical Modeling with Python, in: Proceedings of the 9th Python in Science Conference, 2010, pp. 92–96. doi:10.25080/Majora-92bf1922-011.
URL https://conference.scipy.org/proceedings/scipy2010/seabold.html
[27] Ø. Gabrielsen, T. Liengen, G. Rørvik, S. Molid, T. Stavang, Corrosion Experience with Low Carbon Steel R4 Grade Mooring Chain, in: Offshore Technology Conference, no. OTC-31233-MS, OTC, 2021. doi:10.4043/31233-MS.
URL https://onepetro.org/OTCONF/proceedings/21OTC/3-21OTC/D031S034R005/466513
[28] DNV GL, Offshore Standard - Offshore mooring chain (DNVGL-OS-E302), Edition July 2015 (2015).
[29] K. Bury, Statistical Distributions in Engineering, Cambridge University Press, 1999. doi:10.1017/CBO9781139175081.
URL https://www.cambridge.org/core/product/identifier/9781139175081/type/book
[30] E. N. Lone, T. Sauder, K. Larsen, B. J. Leira, Fatigue reliability of mooring chains, including mean load and corrosion effects, Preprint submitted to Ocean Engineering (2022). doi:https://doi.org/10.31224/2326.